

## REVIEW

©Zhdanov et al.

### PERSPECTIVES FOR THE CREATION OF A NEW TYPE OF VACCINE PREPARATIONS BASED ON PSEUDOVIRUS PARTICLES USING POLIO VACCINE AS AN EXAMPLE

*D.D. Zhdanov<sup>1\*</sup>, Yu. Yu. Ivin<sup>1,2</sup>, A.N. Shishparenok<sup>1</sup>, S.V. Kraevskiy<sup>1</sup>, S.L. Kanashenko<sup>1</sup>, L.E. Agafonova<sup>1</sup>,  
V.V. Shumyantseva<sup>1,3</sup>, O.V. Gnedenko<sup>1</sup>, A.N. Pinyaeva<sup>1,2</sup>, A.A. Kovpak<sup>1</sup>, A.A. Ishmukhametov<sup>2</sup>, A.I. Archakov<sup>1,3</sup>*

<sup>1</sup>Institute of Biomedical Chemistry,  
10 Pogodinskaya str., Moscow, 119121 Russia; \*e-mail: zhdanovdd@mail.ru  
<sup>2</sup>Chumakov Federal Scientific Center for Research and Development  
of Immune-and-Biological Products of Russian Academy of Sciences,  
8/1 Moskovsky settlement, Polio Institute settlement, Moscow, 108819 Russia  
<sup>3</sup>Pirogov Russian National Research Medical University,  
1 Ostrovityanova str., Moscow, 117997 Russia

Traditional antiviral vaccines are currently created by inactivating the virus chemically, most often using formaldehyde or  $\beta$ -propiolactone. These approaches are not optimal since they negatively affect the safety of the antigenic determinants of the inactivated particles and require additional purification stages. The most promising platforms for creating vaccines are based on pseudoviruses, i.e., viruses that have completely preserved the outer shell (capsid), while losing the ability to reproduce owing to the destruction of the genome. The irradiation of viruses with electron beam is the optimal way to create pseudoviral particles. In this review, with the example of the poliovirus, the main algorithms that can be applied to characterize pseudoviral particles functionally and structurally in the process of creating a vaccine preparation are presented. These algorithms are, namely, the analysis of the degree of genome destruction and coimmunogenicity. The structure of the poliovirus and methods of its inactivation are considered. Methods for assessing residual infectivity and immunogenicity are proposed for the functional characterization of pseudoviruses. Genome integrity analysis approaches, atomic force and electron microscopy, surface plasmon resonance, and bioelectrochemical methods are crucial to structural characterization of the pseudovirus particles.

**Key words:** pseudovirus; poliomyelitis; vaccine; inactivation; functional characterization; structural characterization

**DOI:** 10.18097/PBMC20236905253

## INTRODUCTION

The COVID-19 pandemic forced the vaccine researchers and the entire pharmaceutical industry to find rapid solutions to stop the spread of SARS-CoV-2. Bioinformatics methods and techniques were critical to the development of COVID-19 vaccines. Modern bioinformatics and genetic technologies have enabled the rapid acquisition of genome sequences of a new pathogen, allowing the identification of the primary antigenic determinants of SARS-CoV-2 through homology with its predecessors, SARS-CoV and MERS. These data were needed to develop essential mRNA- and vector-based vaccines. In addition, computational analysis and modeling tools have enabled the creation of chimeric genetic structures underlying mRNA and vector vaccines and demonstrated their stability and efficacy [1].

In addition to vaccines generated using bioinformatics methods and novel technologies (mRNA and vector vaccines), a whole distinct cluster of vaccines based on viral capsid protein molecules is being developed [2]. Subunit (based on specific viral proteins or domains) and peptide (based on tiny epitope regions of viral proteins) vaccine platforms are included

in this category [3, 4]. Whole virion platforms based on pseudoviral particles are one of the most promising platforms for vaccine development [5, 6]. A pseudoviral particle is defined as a viral particle that contains the core/base and envelope proteins of one or several viruses. In this case, the genetic material within the pseudovirus must be destroyed to prevent virus from replicating and being pathogenic. In addition, the retention of antigenic determinants should ensure immunogenicity. Pseudoviral particles ought to be distinguished from inactivated ones. Inactivated viral particles (and, therefore, vaccines based on them) are particles that are unable to replicate due to a chemical or physical action. Such treatments usually damage the structure of the virus protein coat, making it different to the original virus. Pseudoviral particles (and vaccines based on them) are a type of inactivated particles that has retained its outer shell but lost its ability to replicate due to genome destruction. A pseudoviral particle by definition is a perfect inactivated virus.

Pseudovirus vaccines are characterized by their safety in use and production, controlled antigen dosage, and efficacy, which is directly dependent on the correct conformation and properties of the antigenic determinants in the vaccines [7].

One of the major challenges in the rapid inactivation of viral particles that can be used to produce vaccines is finding ways for complete inactivation of the genetic material and preservation of the antigenic (immunogenic) properties of the pseudoviral particle. It is necessary to destroy nucleic acids but preserve the protein architectures of pseudoviruses. At the same time, inactivation methods must meet high production requirements (several tons per shift). Due to low production rates and the use of hazardous compounds such as formaldehyde and  $\beta$ -propiolactone, chemical methods are often not suitable [8, 9]. In addition, antigenic determinants may not be effectively retained (or even eliminated) due to intermolecular interactions between amino acids [10].

In this context, various types of the ionizing radiation are more effective than chemical inactivation. The ionizing radiation-based methods destroy viral nucleic acids to prevent the viral replication capacity but preserve viral proteins for generation of antibodies against the resulting pseudovirus [11]. This effect is based on the fact that a large nucleic acid molecule is easier to destroy than a protein molecule; at the same time, the virus usually contains many identical copies of the same protein, and any damage to one of them will not have a significant negative effect on the protein component of the virus.

It is useful to begin research on the production of pseudoviral vaccine particles with a model virus that has sufficient data on its structure and functions. Poliovirus and its attenuated vaccine strains Sabin type 1, 2 and 3 are ideal for this purpose. The advantage of working with these strains is their safety due to the strong population immunity to these strains in the Russian Federation [12, 13]. This virus is one of the most studied ones; therefore, the obtained results can be interpreted using the current knowledge about the characteristics of this virus.

Algorithms adapted to the poliovirus for the determination of residual infectious activity and immunogenicity, as well as algorithms for genome inactivation and integrity analysis of antigenic determinants, can be used to develop and produce other vaccine preparations based on pseudoviral particles.

In this review we have considered the functional and instrumental properties of variously inactivated pseudoviral particles as a potential platform for vaccine development.

## 1. POLIOMYELITIS VIRUS: STRUCTURE AND PROPERTIES AND INACTIVATION

Poliovirus (or poliomyelitis virus) is an enterovirus of the picornavirus family. The viral particle is 27-30 nm in size and it lacks a lipoprotein envelope. The icosahedral capsid has an unsegmented, single-stranded (+)RNA genome of 7441 nucleotides [14]. Three poliovirus serotypes exist and each poliovirus

serotype causes neutralizing antibody generation. However, a virus of one serotype cannot be neutralized by antibodies against two other serotypes [15]. Human and primate cells replicate poliovirus. Vero cell culture is one of the best-known cell cultures used to propagate poliovirus and produce polio vaccines [16].

The poliovirus capsid consists of four proteins: VP1, VP2, VP3, and VP4, each of which has 60 copies in a viral particle [17] (Fig. 1).

Viral structural proteins form several symmetrical structures on the surface of the particle: "propeller", "star" ("mesa"), and "canyon". The most exposed portions serve as antigenic sites for antibody formation. Because the "canyon" is essential for particle binding to the viral receptor, the areas around it are critical to produce effective neutralizing antibodies [18]. There are four antigenic sites involved in the production of poliovirus neutralizing antibodies. One of the most important sites is formed by the BC loop of the VP1 protein chain, which is a part of the "mesa" structure [19].

The D antigen refers to the capsid structure of an infectious poliovirus particle; it represents a set of conformational antigenic sites required for the development of neutralizing antibodies that inhibit interaction with the cellular CD155 receptor (PVR). The so-called H or C poliovirus antigen is a structural antigen that does not cause the formation of neutralizing antibodies and is formed after the infectious particle is restructured during thermal or other treatment or as a result of virus binding to the receptor followed by subsequent introduction of genomic RNA into the cytoplasm. Thus, the primary issues to be addressed in the inactivation process are the preservation of the spatial structure of the D antigen and the development of algorithms to control its integrity [20, 21].

Currently, attenuated Sabin vaccine strains of poliovirus types 1 and 2 are used: type 1 — LSc 2 ab, type 2 — P712 Ch 2 ab, and type 3 — Leon 12a1b. Sabin strains 1 and 3 are the basis of the live polio vaccine in the Russian Federation. Sabin strain type 2 was part of the trivalent live polio vaccine used in the USSR and former Soviet Union territories for more than 40 years. These strains are attenuated, i.e., they cannot be the cause of disease in a healthy person.

The introduction of the WHO polio eradication program in the late 20th century restricted the use of live polio vaccine in world regions without natural circulation of wild-type poliovirus. Vaccine strains can quickly regain neurovirulence in the human body during reproduction. At the same time, the WHO has identified a trend toward the development of inactivated vaccines based on attenuated Sabin strains to replace the currently used wild-type poliovirus vaccines. The development of effective vaccines based on Sabin strains is one of the major goals for global polio eradication [22, 23]. The antigenic determinants

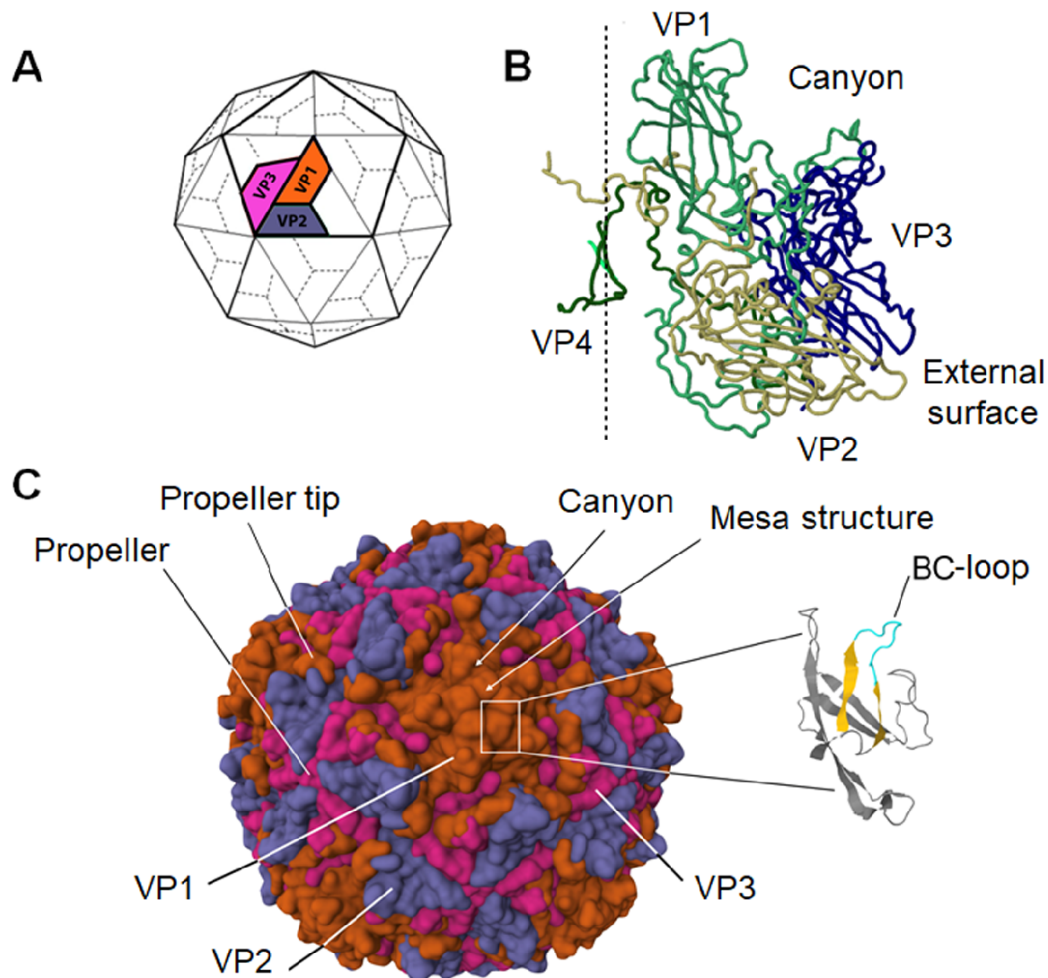


**Figure 1.** The structure of the poliovirus virion. (A) Protein composition of the virion surface. (B) Structure of the canyon-forming capsomere. (C) Structure of the virion surface and the BC loop of the VP1 protein, based on the Protein Data Bank data source 1PVC. The color version of this figure is available in the electronic version of the article.

of the virus responsible for the generation of protective immunity have been found, and their infectious properties have been studied during many years of research around the world. At the Chumakov Federal Scientific Center for Research and Development of Immunobiological Drugs of the Russian Academy of Sciences (Polio Institute) in the Russian Federation, the full cycle of poliovirus research was carried out, beginning with the basic principles of the course of viral infection and ending with the industrial development of the pathogen with the subsequent production of vaccine preparations.

The Polio Institute has developed technologies for large-scale production of poliovirus in bioreactors and validated tests to analyze the amount of viral antigen in samples. Oral live and inactivated polio vaccines have been developed based on Sabin strains [23–25].

There are several methods of virus inactivation that are currently used to produce inactivated vaccines. They are divided into two types based on the type of treatment: physical (heat treatment, ultraviolet light, and gamma irradiation) and chemical

treatments. Physical methods include ultraviolet light and gamma irradiation, while chemical methods include formaldehyde and  $\beta$ -propiolactone [26, 27]. None of these methods has a clear advantage in terms of preservation of antigenic determinants (i.e., the use of formaldehyde) or process safety requirements (i.e., gamma irradiation).

Inactivated vaccines are often preferred over other forms of vaccines for safety reasons; however, certain problems may arise due to inadequate virus inactivation. This can lead to cases of post-vaccination disease or destruction of virus-neutralizing epitopes, resulting in poor production of virus-neutralizing antibodies [28].

The two most common types of chemical reagents used as inactivators are reticulating (disintegrating) agents and alkylating agents. Aldehydes such as formaldehyde, glutaraldehyde, and glycidaldehyde are reticulating agents. Formaldehyde is the most commonly used.  $\beta$ -Propiolactone, ethyleneimine, and other aziridines are alkylating agents. The mechanism of action of the inactivating chemical reagents includes their interaction with nucleic acids and proteins [29].

Virus inactivation is based on two mechanisms: changes in proteins interacting with cellular receptors (including the development of cross-links between individual components) and loss of nucleic acid replication ability. The required concentration of inactivating agents is mostly determined by the relative concentration of proteins and nucleic acids in the inactivation medium, which poses technological challenges for the industrialization of this process. The temperature and homogeneity of the inactivated substrate also play an important role in the kinetics of virus inactivation [30, 31]. Although inactivation by chemical reagents has been optimized for poliovirus, nevertheless it has a negative impact on D antigen retention.

1.1. Formaldehyde for Virus Inactivation

A concentrated 37% solution of formaldehyde in water (formalin) is commonly used for vaccine production [32]. Low molecular weight formaldehyde readily penetrates cell membranes and viral capsid proteins and affects both enveloped and non-enveloped viruses [33].

Formaldehyde interacts more rapidly with amino groups in amino acids and proteins (with formation of methylol derivatives) than with nitrogenous bases of nucleic acids. Formaldehyde has been shown to react with a variety of amino acid residues under a wide range of conditions, yielding hydroxymethylated, cyclized, N-methylated, and N-formylated compounds with varying degrees of stability (Fig. 2). [34].

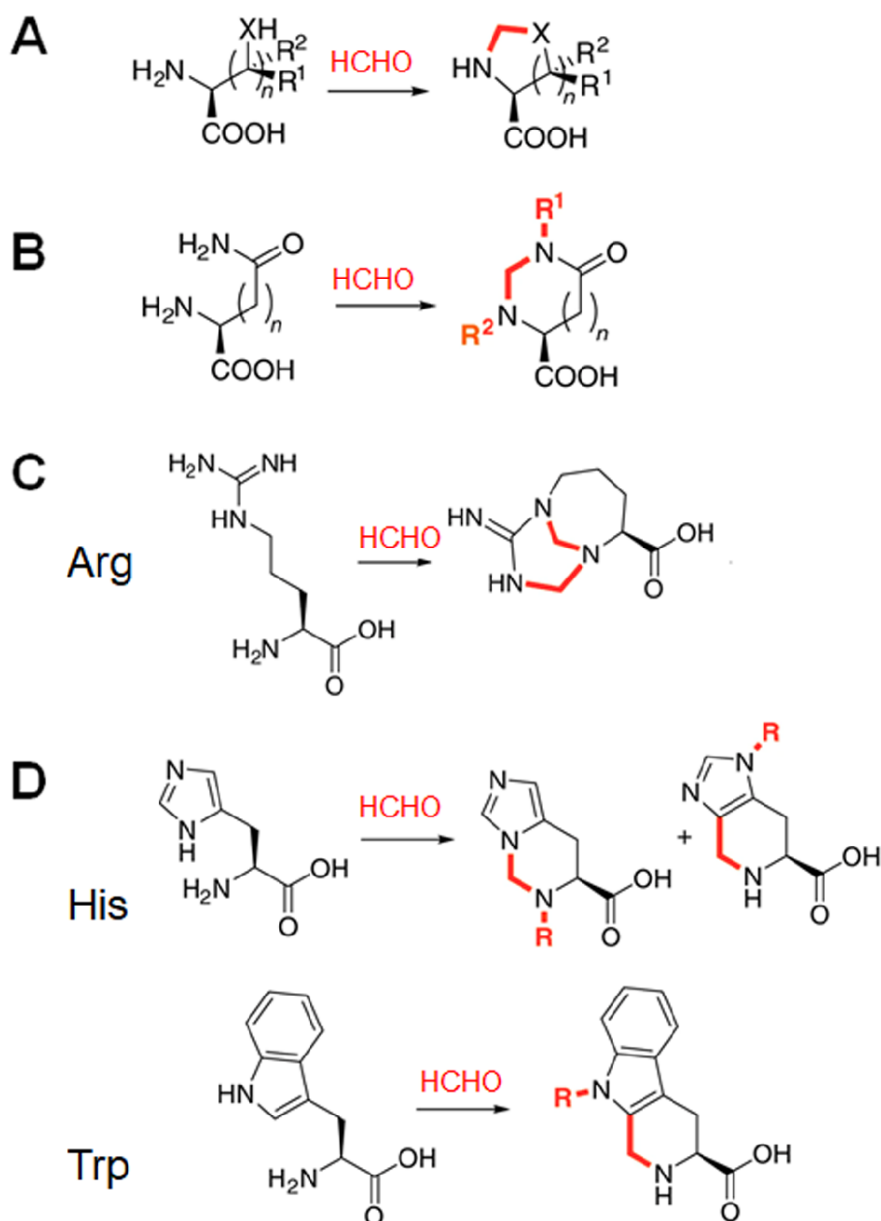


**Figure 2.** Stable products of the interaction of formaldehyde with (A) sulfur- and OH-containing amino acids (X – S or O; R – Me or H), (B) asparagine and glutamine (R – H or  $\text{CH}_2\text{OH}$ ), (C) arginine, (D) aromatic amino acids, histidine and tryptophan (R – H or  $\text{CH}_2\text{OH}$ ).

The addition of formaldehyde to amino groups of purines and pyrimidines reduces the activity of the nucleic acid template by creating cross-links — methylene bridges (Fig. 3A). Formaldehyde-induced amino acid modifications result not only in the fixation of single residues but also in the cross-linking of amino acids positioned close together in the spatial structure of the macromolecule (Fig. 3B).

The products of the formaldehyde-amino acid interaction can react more rapidly with nucleic acids than formaldehyde itself. The major reaction products then slowly engage additional protein groups, culminating in the formation of covalently bound

polypeptide dimers. At the same time, the protein shell becomes denser, and its permeability decreases, slowing the inactivation of the viral genetic material. It should be emphasized that the reaction of formaldehyde with amino groups is reversible, which means that the activity of the nucleic acid can be restored by removing the excess reagent or diluting the solution [33].

Due to the above-mentioned aspects of the mechanism of interaction of formaldehyde with the virus, certain inactivated vaccines contain incompletely inactivated virus particles, which may lead to outbreaks of viral infections during

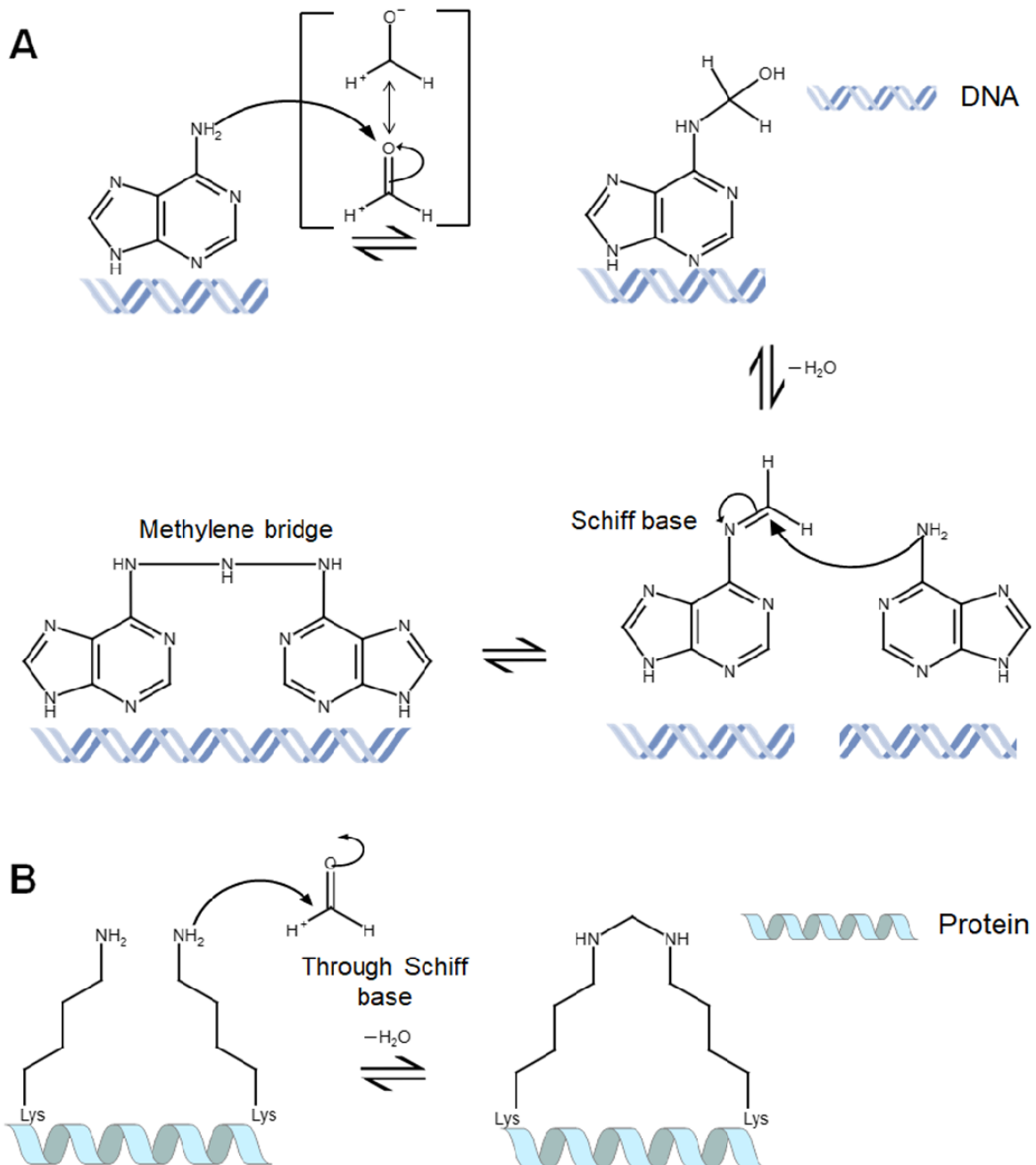


**Figure 3.** Reactions of formaldehyde with nucleic acids and amino acids. **(A)** Interaction with adenines results in formation of a methylene bridge or Schiff bases. **(B)** Interaction with the amino groups of lysine residues of viral capsid proteins in the monohydroxymethylation reaction and formation of a methylene bridge.

vaccination. This has been reported for several viruses, including foot-and-mouth disease virus (FMDV) and Venezuelan equine encephalitis virus (VEEV). Molecular analysis has shown that FMD epidemics in Western Europe in the 1980s and VEEV in Central America in the 1970s were caused by inactivated virus vaccinations [28].

The unfavorable effect of formaldehyde on the antigenic structure of a number of viruses is a major drawback to its use as an inactivating agent [35]. Treatment with formaldehyde has been shown to alter the antigenic structure of poliovirus. Formaldehyde promotes damage to the immunodominant epitope (site 1) in the BC-loop of Sabin type 1 poliovirus [36]. This has also been demonstrated for other viruses, including herpes virus 1, Newcastle disease virus, influenza virus, and Rift Valley fever virus [9].

The presence of free formaldehyde in the inactivated whole virion H1N1 influenza virus vaccine inhibited monoclonal antibody (mAb) formation against conserved influenza virus epitopes [37].

Chemical changes induced by formaldehyde are influenced by such parameters as incubation time, pH, temperature, formaldehyde concentration and ionic strength of the solution. The duration of the inactivation process has a detrimental effect on the safety and activity of the target viral antigen, as well as the immunogenicity of the inactivated vaccine. Therefore, appropriate selection of inactivation conditions is critical in the production of an inactivated vaccine [33].

The toxicity of formaldehyde is another limitation of this inactivation approach. Depending on the type of vaccination, this chemical must be eliminated, diluted, and/or converted to a nontoxic form after processing [38].

### 1.2. $\beta$ -Propiolactone for Virus Inactivation

$\beta$ -Propiolactone is another inactivating agent widely used by vaccine manufacturers. It has a four-carbon ring and is a member of the lactone family. Virus inactivation is generally caused by irreversible alkylation of nucleic acid bases (Fig. 4); this limits viral genome

replication or, may cause viral genome destruction.  $\beta$ -Propiolactone inactivation has a stronger effect on enclosed viruses than on non-enveloped viruses [39].

It should be noted that the initial alkylated products can act as reagents in subsequent cross-linking reactions. These include cross-linking of amino acid residues of the protein capsid, interstrand DNA cross-linking, and the formation of loops within the viral RNA (intrastrand RNA cross-linking) [39, 40].

Certain evidence exists in the literature that, unlike formaldehyde,  $\beta$ -propiolactone inactivates viruses primarily by altering their nucleic acids and therefore the antigenic structure of viruses is likely to be retained after  $\beta$ -propiolactone inactivation [41].

On the other hand,  $\beta$ -propiolactone was found to form *bis*-alkylated complexes due to the formation of inter- and intramolecular cross-links in proteins (especially at high doses). For example, in the case of influenza viruses, the hemagglutinin activity and the enzymatic activity of neuraminidase can be greatly reduced but not destroyed [28].

The immunogenicity study of formaldehyde- and  $\beta$ -propiolactone-inactivated vaccines, has shown that immunization of mice with a whole-virion H5N1 influenza virus vaccine inactivated by  $\beta$ -propiolactone resulted in successful protection against H1N1 virus compared to its formaldehyde-killed equivalent. These results demonstrate that the structure of viral proteins is conserved during  $\beta$ -propiolactone inactivation due to appropriate inactivation conditions [42].

Another study, performed using polyacrylamide gel electrophoresis (PAGE), has shown that inactivation of the coronavirus SARS-CoV-2 was accompanied by appearance of dispersive bands and cross-links in the S protein [43]. Compared to  $\beta$ -propiolactone treatment, the antigen concentration demonstrated a 2-fold decrease within 20-24 h. The virus particles were very homogeneous after  $\beta$ -propiolactone treatment. It should be noted that long-term treatment with  $\beta$ -propiolactone (48 h) can cause viral aggregation and an increase in viral particle size up to 150 nm with simultaneous decrease in the surface antigen concentration [43].

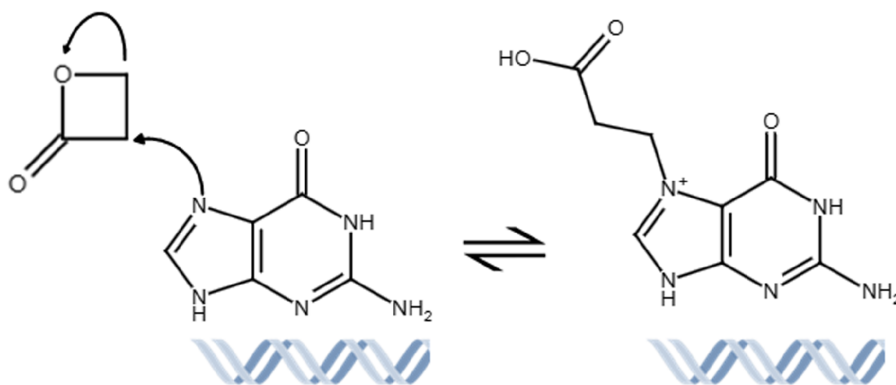


**Figure 4.** The interaction of  $\beta$ -propiolactone with nucleic acids causes alkylation of bases, e.g., guanine.

Potential disadvantage of  $\beta$ -propiolactone consists in its carcinogenic properties, although products of its hydrolysis are not carcinogenic.  $\beta$ -Propiolactone has the potential advantage of reacting with nucleic acids, so any contaminating genetic material obtained from a cell culture should be inactivated as well. The use of  $\beta$ -propiolactone as the inactivating agent has several advantages over formaldehyde: (i) inactivation takes an average of 24 h, compared to more than a week needed for formaldehyde; (ii) it can be hydrolyzed after completion of the inactivation process; (iii) inactivation of contaminating nucleic acids from producer cells, facilitates the process of subsequent purification.  $\beta$ -Propiolactone can be quickly hydrolyzed to harmless byproducts. During the inactivation process,  $\beta$ -propiolactone is hydrolyzed to 3-hydroxypropionic acid, which is an intermediate of human lipid metabolism [8, 44].  $\beta$ -Propiolactone has been increasingly used in recent years due to its precise targeting of viral genomes [45].

### 1.3. Ultraviolet Light (UV) for Virus Inactivation

The use of UV radiation is one of the physical means of inactivating viruses. Based on the wavelength range UV radiation is classified into three types: UV-A (320 nm to 400 nm), UV-B (280 nm to 320 nm), and UV-C (200 nm to 280 nm). Most of the inactivating effects occur in the UV-C spectrum, with a small amount occurring in the UV-B region. The virus-inactivating effect of UV radiation is primarily related to the activation of photodimer formation between adjacent pyrimidine bases (Fig. 5); this leads to the disruption of viral replication and transcription in host cells. UV radiation with a wavelength of 254 nm (in the UV-C spectral band) is commonly used to inactivate viruses [28].

Although nucleic acids are the primary targets, UV irradiation can create cross-links between the viral genome and capsid proteins via the photochemical interaction of amino acid residues (particularly cysteine) with uracil and/or thymine. UV light can also induce structural changes in viral capsid proteins, resulting in the formation of a photoproduct. UV light has a slower effect on viral proteins than on nucleic acids. Long-term exposure not only

increases this damage but also promotes oxidative damage, such as the formation of carbonyl groups in capsid-protein amino acids and this reduces the immunogenicity of the virus particles [46].

### 1.4. Gamma and Accelerated Electron Irradiation for Virus Inactivation

Gamma irradiation is a type of high-energy, low-dose-rate ionizing radiation often used to sterilize and inactivate bacteria [47, 48]. This type of radiation has enough energy to displace (or even eliminate) the outer electrons of molecules, resulting in the breakdown of covalent bonds and ionization [48]. Unlike UV radiation, gamma rays penetrate deeper and can be used to inactivate viruses in large quantities [47]. According to the radiation target theory, viral genomes are more susceptible to structural damage from gamma rays than viral proteins due to their higher molecular weight [48]. Oxidative damage, particularly changes in surface epitopes such as carbonylation of viral proteins and, to a lesser extent, viral genome destruction, reduce the antigenicity of viral particles and thus the effectiveness of vaccination [33].

To limit the generation of free radicals by minimizing radiolysis of water, gamma-ray inactivation of viruses should be performed in a frozen state [47]. Frozen virus samples are kept on dry ice during irradiation. The effect of gamma radiation on this inactivation approach depends largely on the type and degree of viral genome abnormalities, such as single- and double-strand breaks, cross-linking, and nucleotide degradation. This feature distinguishes gamma radiation from the previously mentioned approaches [33]. The demanding requirements for the conditions of the infrastructure organization of the radiation protection system, staff competence and logistic chains are significant drawbacks of gamma irradiation. As a result, the focus has been shifted to accelerated electron irradiation. Accelerated electron irradiation has the same advantages as gamma irradiation but does not require such stringent infrastructure conditions. In this regard, accelerated electron irradiation has been proposed as the most adequate method for producing pseudoviral particles.

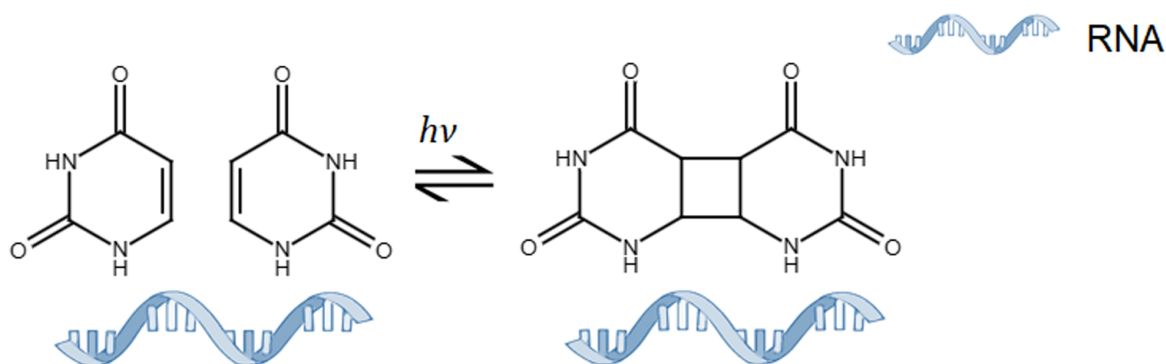


**Figure 5.** Formation of a pyrimidine (uracil) dimer under the influence of ultraviolet radiation.

2. FUNCTIONAL CHARACTERISTICS OF PSEUDOVIRAL PARTICLES

When developing whole-virion vaccines using polio virions as the starting material, research on the characteristics of the resulting particles plays an important role. The basic goals of studying pseudoviral particles, as well as any inactivated particles obtained from infectious particles by depriving them of replication potential, are to determine the completeness of inactivation, antigen content, and immunogenic activity. The determination of inactivation completeness (residual infectivity) is the most important technique as it helps to select optimal settings for viral particle inactivation and thus represents a basis for the safety of the developed vaccine. The determination of antigen concentration and immunogenic activity allows to determine the optimal technique for virus inactivation while preserving the structure of the viral protein envelope and sets the stage for drug success.

2.1. Determination of Residual Infectious Activity

The infectivity test for viral particles developed at the Polio Institute indirectly analyzes disruptions in the genetic material or structure of the entire pool of particles that have been subjected to an inactivation

technique that has resulted in the loss of viability of the viral agent. The analytical procedures are designed to demonstrate that the processed viral material does not contain particles capable of causing viral infection. The poliovirus is a lytic virus that causes cell death [49]. The analysis of a residual infectious activity is based on the visual detection of its lytic activity. For this purpose cell cultures sensitive to poliovirus infection and promoting effective virus replication are used [50].

Cell sensitivity to the polio virus is determined by the presence of a virus-specific receptor, PVR or CD155, which is expressed in a fairly limited number of human and great ape cell cultures [51]. Primary cultures of primate cells, such as green monkey kidney cells, have traditionally been used by researchers. However, as cellular technologies have advanced, continuous cell cultures of human and non-human primates have become popular: HEP-2, L20B, Vero, and others. Based on studies of the sensitivity of these cultures to poliovirus, it was found that they could be used to perform assays to look for residual infectious particles and assess their concentration [52, 53].

The viral dose was measured by titration on a sensitive Hep-2 cell culture at 50% infectious dose (TCID<sub>50</sub>) to determine the concentration of infectious poliovirus particles (Fig. 6).

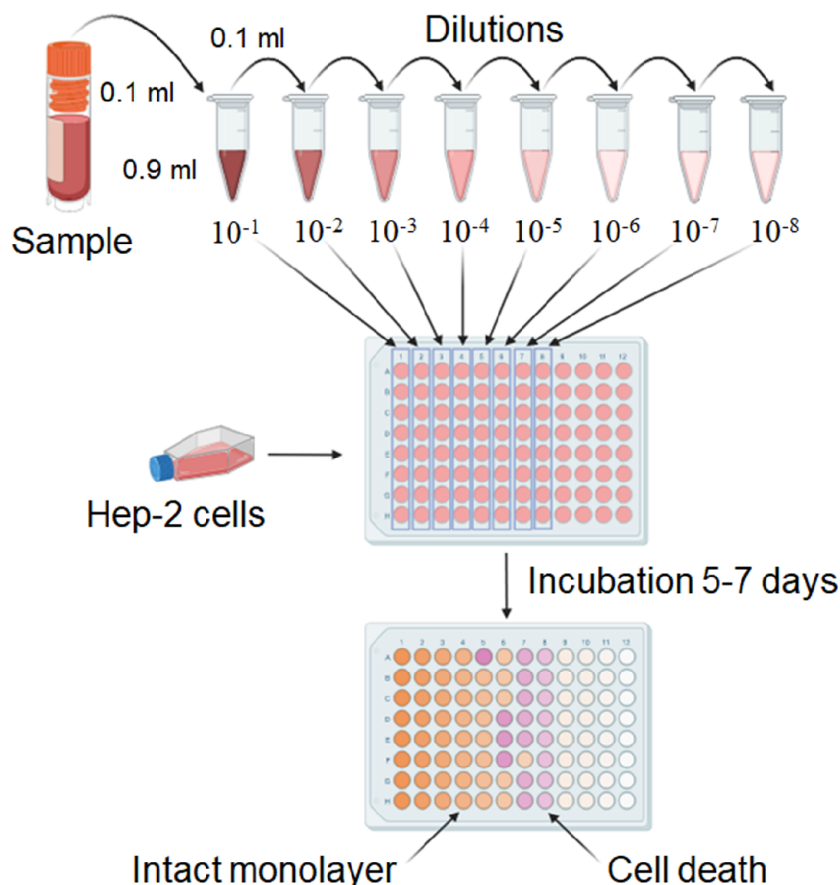


**Figure 6.** The scheme illustrating the procedure for titration of samples using a sensitive cell culture. The procedure consists of preparing serial dilutions of the sample in a cell culture medium, adding the sample dilutions to a 96-well plate containing a Hep-2 cell culture, incubating for 5-7 days, and reading the results.

The developed algorithm is based on determining the content of infectious particles by mixing a suspension of sensitive Hep-2 cells with different dilutions of the test material in several replicates: from undiluted substance to  $10^{-(N+2)}$  dilution, where  $10^N$  TCID<sub>50</sub>/ml is the titer of the original noninactivated poliovirus.

After inactivation, incubation of the test substance with a sensitive cell culture (in the case of poliovirus — Hep-2, L20B, or Vero) is used as the last step of proving the absence of infectious virus particles by two consecutive passages for 7 days each, in accordance with WHO and European Pharmacopoeia recommendations (Fig. 7). The developed algorithm detects residual “traces” of virus that have not been inactivated. As poliovirus multiplies, selected cell cultures die, and the presence or absence of live virus particles in the sample is assessed by the status of the cell monolayer. The state of the monolayer in comparison with the control culture is used to evaluate the cell culture during passages. After successive passages, during which even a single particle capable of multiplying increases in number and causes cell death, it is possible to finally determine the conditions for complete inactivation of the poliovirus upon irradiation (Fig. 7) [52, 54, 55].

## 2.2. Determination of Immunogenicity

Immunoassay methods using antibodies to the D antigen are used to provide a preliminary assessment of antigenic characteristics that indirectly indicate the safety of determinants on the surface of inactivated poliovirus particles. In assessing the potential efficacy of inactivated polio vaccines, radial immunodiffusion was first used to estimate the D antigen concentration. The test antigen is diffused in an agar medium containing specific antibodies. The size of the diffused “ring” in the sample correlates with the concentration of the antigen [56]. Immunodiffusion has been replaced by the enzyme-linked immunosorbent assay (ELISA), which compares the level of immunogenic poliovirus

D antigen in a sample with a known immunogenic standard sample [57]. ELISA is an important method for the characterization of vaccines and other drugs that detects the presence of antigens (Fig. 8).

Better evaluation of the effectiveness of the interaction of inactivated particles with antibodies to the D antigen of poliovirus (i.e. with neutralizing antibodies) can be achieved using surface plasmon resonance-based biosensors (see Section 3.4).

The described methods indirectly assess the similarity of inactivated particles with native live poliovirus particles by interaction with neutralizing antibodies. The stronger contact implies that the structure of the antigenic site remains intact and therefore the inactivated particle is thus more effective in generating protective antibodies in response to these structural features during immunization.

ELISA is currently a widely used technology for identification of the D antigen in the production of inactivated polio vaccines; it is required to control such parameter as specific activity. Specific activity is one of the most important measures of vaccine quality [58], which is expressed in D antigen units (DU/ml or DU/dose).

There are many variations of the ELISA technique for determining D antigen levels, utilizing different antigen-antibody interaction patterns and monoclonal and polyclonal antibody types. Each laboratory uses unique antibodies and ELISA procedures to measure D antigen levels. The antibodies must be specific to the poliovirus serotype and the D antigen [59]. The problem of standardization of D antigen assay is determined by the complex antigenic nature of poliovirus and the wide range of ELISA systems available worldwide [60]. Laboratories must use an international standard, or an internal standard calibrated against an international standard that has been assigned a specific number of D antigen units (DU) to ensure comparability of results. It is possible to express the efficacy of preparations from different manufacturers using the same units [59]. The high specificity of antibodies is the key factor

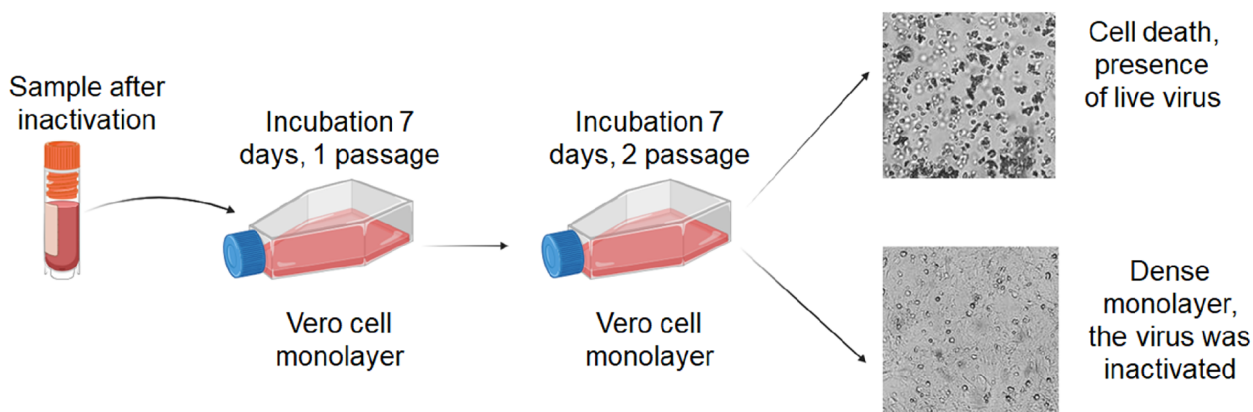


**Figure 7.** The scheme illustrating the proposed algorithm for passage of inactivated material to test the residual infectivity.

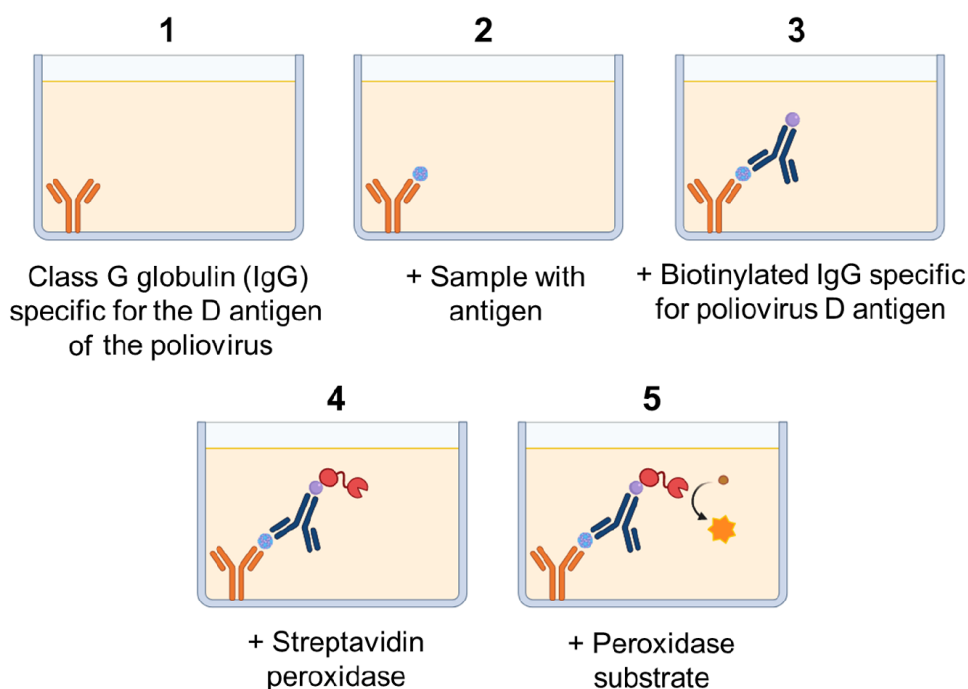


**Figure 8.** Schematic of an adapted enzyme-linked immunosorbent assay for the determination of poliovirus D antigen in samples.

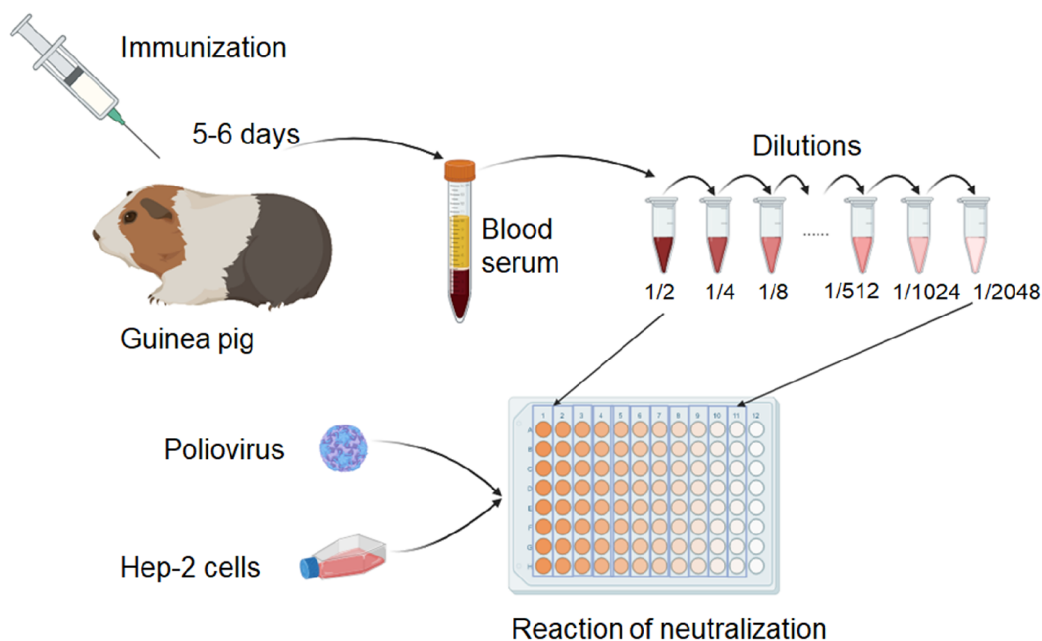


**Figure 9.** The scheme showing the assessment of immunogenicity.

for effective ELISA procedure. Denatured poliovirus antigen (H antigen), which lacks protective immunity, is easily generated from native poliovirus antigen (D antigen). Therefore, only the composition of the D antigen should be used to assess vaccine efficacy [57].

IgG specificity for the D antigen was at least ten times better than for the H antigen, according to an ELISA test technique based on rabbit polyclonal sera. The assay is based on biotin-conjugated antibodies isolated from rabbit immune serum [57, 58] (Fig. 8).

Analysis of the D antigen content allows early assessment of the immunogenic properties of the viral particle. Immunogenicity, or the ability of an inactivated material to induce the production of neutralizing antibodies, is assessed directly by immunizing animals (guinea pigs and rats) and then determining levels of neutralizing antibodies in the blood (Fig. 9) [61].

The higher the concentration of neutralizing antibodies in the blood of immunized animals, the more effective the inactivated sample will be under the same experimental conditions.

### 3. STRUCTURAL AND BIOCHEMICAL CHARACTERISTICS OF PSEUDOVIRAL PARTICLES

The residual infectious activity and immunogenicity of the resulting pseudovirus are directly dependent on inactivation (inability to replicate) and preservation of antigenic sites. Impaired replication activity is associated with disruption of the viral genetic material. Therefore, assessment of the genome integrity of pseudoviral particles is an important step in selecting inactivation conditions. The preservation of antigenic determinants is followed by a change in viral particle structure. Therefore, the study of structural and biochemical properties, which allow the assessment of the degree of inactivation and the structure of the pseudovirus, is essential.

#### 3.1. Pseudovirus Genome Integrity Analysis

The degree of genome degradation determines the efficiency of virus inactivation during vaccine development. The genome of the Sabin 1 poliovirus strain is represented by 7441 nucleotides of single-stranded RNA with template activity (positive or +RNA), i.e., RNA that can be directly translated by an infected cell.

Quantitative polymerase chain reaction (real-time PCR) is a method of virus and pseudovirus genome integrity assessment proposed by the research group at the Institute of Biomedical Chemistry (IBMC) [62–64]. The principle is based on the repeated selective copying of a specific fragment of DNA using the enzyme DNA polymerase [65, 66]. In quantitative PCR, changes in the amount of a specific PCR product (amplification of a region of the viral genome) labeled with a fluorescent probe are monitored

during each reaction cycle [67–69]. PCR requires a reverse transcription process (RT-PCR) because the poliovirus genome consists of RNA.

We hypothesize that inactivation of the virus by chemical or physical means will damage the nucleic acid molecule, negatively affecting the efficiency of RT-PCR and the number of intact amplifications. Such damage will increase the cycle at which amplification is observed when performing real-time RT-PCR. In other words, a higher number of the PCR cycle at which amplification is detected corresponds to an increase in viral genome degradation (Fig. 10). Real-time RT-PCR cycle thresholds (Ct) are defined as the number of amplification cycles needed for the cumulative fluorescence (resulting from target DNA amplification) to exceed a threshold value. As a result, Ct values are inversely proportional to viral genome stability; low Ct values indicate genome integrity, whereas high Ct values indicate significant nucleic acid degradation [70]. The RNA of the intact virus was used as a reference.

#### 3.2. Analysis of the General Morphology of Pseudoviral Particles

##### 3.2.1. Scanning electron microscopy (SEM).

SEM is a type of electron microscopy that detects secondary electrons (SE), backscattered electrons (BSE), and transmitted electrons (scanning transmission electron microscopy, STEM).

A tightly focused electron beam scans the surface of the specimen or “draws a raster” over a region while simultaneously recording various signals produced by the interaction of the primary electron beam with the specimen (Fig. 11). To generate

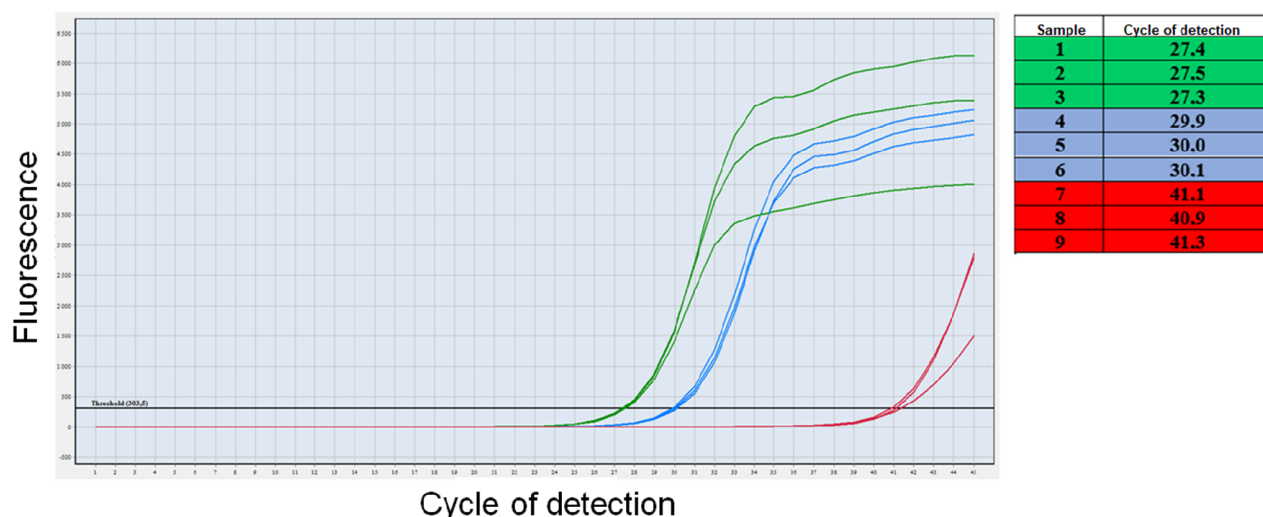


**Figure 10.** Detection cycles of real-time RT-PCR amplifications of poliovirus samples inactivated by electron irradiation. An increase in the radiation dose and damage to the RNA structure are accompanied by an increase in Ct. Samples n. 1-3 are cycles for non-inactivated control samples (green lines); samples 4-6 are cycles for virus samples irradiated at a dose of 10 kGy (blue lines), and 7-9 are cycles for virus samples irradiated at a dose of 30 kGy (red lines). The color version of this figure is available in the electronic version of the article.

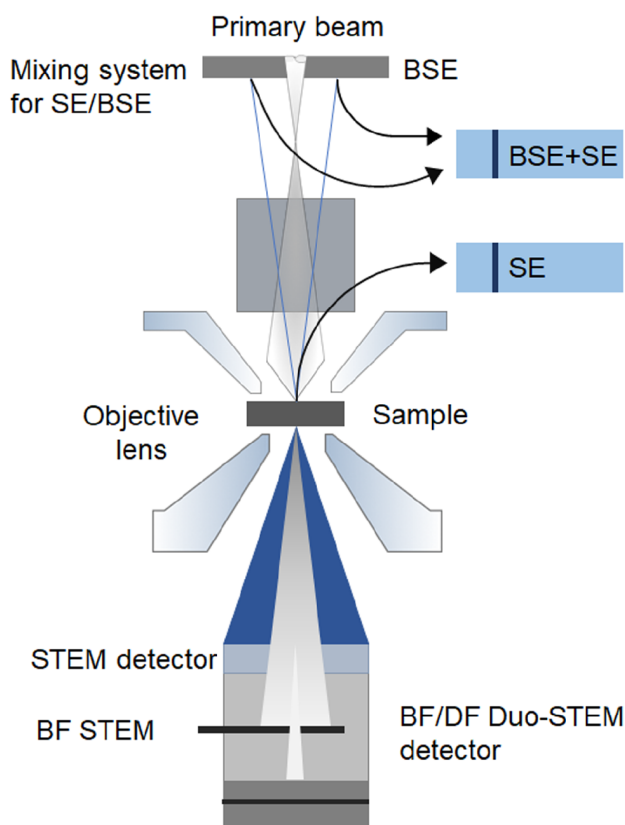


**Figure 11.** The Hitachi S-5500 scanning electron microscope detector system. The production of secondary and reflected electrons is caused by the primary beam, which is produced by a set of focusing lenses. The SE detector (labeled on the right) collects low-energy secondary electrons and is located off-axis from the SEM. Above the specimen is the high-energy reflected electron detector BSE. The number of reflected electrons is much smaller than the number of secondary electrons, so this model uses an SE/BSE signal mixing technique to maximize sensitivity to reflected electrons. A separate SE detector captures secondary electrons produced in the BSE detector. A STEM detector detects electrons passing through the sample. This detector is divided into two sections: a bright field detector (BF STEM) and a dark field detector (BF/DF Duo STEM detector).

the primary beam, a scanning microscope typically uses an accelerating voltage in the range of  $500 \text{ V} \div 30 \text{ kV}$ . A detector of a specific design is used to register each type of the signal. SE, BSE, and STEM detectors are the most commonly used in scanning microscopes [71].

Secondary electrons (SE) are electrons produced as a result of the inelastic contact of the primary electrons with the sample. Secondary electrons typically have energy of less than 50 eV. They can be used to identify the shape of individual particles and surface topography. It is possible to obtain the best resolution by varying the acceleration voltage and beam current to achieve an appropriate relationship between the signal strength and depth of SE generation.

Backscattered electrons (BSE) are electrons produced by the elastic interaction of primary electrons with the nuclei of target atoms; the BSE energy is slightly different from the primary beam energy. Backscattered electrons are sensitive to the atomic number of the target; they allow one to detect the contrast between elements in a sample with different atomic numbers.

Transmitted electrons are electrons from the primary beam that have been detected by a transmission electron detector (STEM) after passing through the material. The contrast that appears is identical to that seen in a transmission microscope [71].

Traditional SEMs often require solid and conductive materials. In addition, the sample chamber must be vacuumed. However, environmental scanning electron microscopy (ESEM) overcomes these limitations by allowing operation in a shallow vacuum, thereby increasing the number of accessible materials, such as those in solution or nonconductive materials [72].

SEM has a typical resolution of 3–5 nm. This means that it cannot measure feature sizes on the same scale as transmission electron microscopy (TEM). Although SEM has a lower resolution than TEM or AFM, it can still be useful in determining the size and shape of pseudoviral particles [73–75]. Dry powder vaccines are commonly used in traditional SEM because they fit the sample requirements of SEM: they are solid and stable under vacuum [76].

However, only ESEM can be used to image other synthetic vaccines that must be preserved in an aqueous environment [77]. To obtain a clean, high-contrast image, samples should be at least 100 microns in size. Despite the limitations of many synthetic vaccines, SEM can provide three-dimensional information about a sample due to depth-of-field phenomena [78]. Figure 12 shows SEM images of inactivated poliovirus particles.

### 3.2.2. Transmission electron microscopy.

The operating principle of a transmission electron microscope is based on the utilization of the wave characteristics of an electron. TEM is comparable to an optical microscope but with wavelengths 100,000 times shorter than visible light wavelengths. This feature of TEM makes it possible to obtain an image of an object, such as the structure of a nanotube or fullerene, with a resolution on the order of the size of an atom. Modern microscopes can distinguish points projections of which are separated by  $0.7 \text{ \AA}$ .

This type of microscopy uses terminology carried over from optics. An electron gun is the source of the electron beam. Magnetic lenses serve as lenses in SEM, and their characteristics, such as spherical and chromatic aberrations are also important for image clarity. Image registration is performed using a CCD camera [79].



**Figure 12.** The SEM image of poliovirus particles deactivated with formaldehyde. The image was obtained at the Avogadro collaborative center at IBMC.

Cryo-electron microscopy (cryo-EM) has formed and rapidly developed during the last decade. Cryo-EM is a specific type of TEM commonly used to visualize biological samples, which are much more susceptible to radiation degradation than inorganic samples. The samples are examined at extremely low temperatures (down to  $-180^{\circ}\text{C}$ ). With cryo-EM, it is possible to obtain images with higher resolution and contrast than with the traditional type of SEM. In cryo-EM, a thin (30 nm) film of amorphous (glassy) water is used as a sample holder (substrate) at a temperature of  $-150^{\circ}\text{C}$ . The glassy state is achieved by rapidly cooling the water film containing the sample (protein molecule, virus, vesicle) so that ice crystals do not have time to form and grain boundaries do not scatter electrons. In addition, low temperatures slow down the movement of free radicals formed during the passage of electrons in the sample, which delays the degradation of biological objects [80].

The highest resolution that can be achieved with cryo-EM is  $2.2 \text{ \AA}$  [81], while for SEM this value is only approximately  $10 \text{ \AA}$  [82]. Cryo-EM has been widely used to reconstruct three-dimensional images and has contributed significantly to the development of structural biology.

TEM has been widely used for virus imaging since 1955, with one of the first publications focusing specifically on imaging poliovirus [83]. In 1965, a detailed study of the dynamics of poliomyelitis virus development in HeLa cells was performed using conventional TEM [84]. Since late 1990s, with the development of cryo-EM, it became possible to study the three-dimensional structure of the virus in detail [85]. In addition, it became possible to study the three-dimensional structure of the virus-receptor-membrane complex using cryo-TEM [86]. These data suggest the existence of separate populations of subcellular vesicles, each playing a specialized role in the processes of poliovirus replication [87].

### 3.3. Atomic Force Microscopy (AFM)

Since its introduction in 1986, AFM has become firmly established in the arsenal of researchers in many areas [88]. High repeatability of results, the ease of sample preparation, and the consistency of results with other methods (such as dynamic light scattering and electron microscopy) “created reputation” of AFM as one of the most actively used methods. Another advantage of AFM images is spatial resolution of around fractions of nanometers.

AFM is a high-resolution surface characterization technique for measuring the shape, height, and mechanical properties of materials placed on a substrate or in a droplet with high resolution. The operating principle of AFM is based on the cantilever deflection induced by physical forces between the cantilever tip and the sample. The force acting on the probe from the surface side leads to cantilever bending (Fig. 13). The appearance of “elevations” or “depressions” under the tip leads to a change in the force acting on the probe, and hence to a change in the amount of cantilever bending [89].

The two most popular AFM modes are: (i) the noncontact mode, in which the tip is detached from the sample surface and the cantilever deflection is caused by attraction or repulsion forces between the tip and the surface, and (ii) the contact mode, in which the AFM tip slides over the surface. The direct mechanical contact of the probe with the surface is the drawback of contact AFM techniques. This often results in destruction of the sample surface during scanning and probe damage. In addition, contact techniques are almost unsuitable for samples with low mechanical stiffness, like biological objects and structures made of organic components. When scanning becomes nearly impossible on such things, the needle is often held too strongly by adhesion forces (the needle sticks). To reduce the destructive force and prevent the probe from sticking, tapping mode modulation was developed. In this mode, an external piezoelectric device operates at a resonant frequency to stimulate cantilever oscillations. The control parameter of the feedback circuit is the amplitude of the cantilever vibrations. Frictional forces and capillary sticking are minimized if the cantilever breaks the established connection with the sample at each period with

an appropriately large amplitude. The tapping mode is most used for the analysis of pseudoviral particles [77, 90].

Although AFM analysis of viral particle morphology is not a routine procedure, it is widely used in scientific research. Several works [91–94] highlighted the potential applications of this analytical approach to the evaluation of the virus particles morphology. In addition to visualization, AFM has been used to study the mechanical properties of viruses [95, 96] and the lytic properties of bacteriophages [97, 98], and to map specific areas of primary viral attachment to cells [99]. In addition, AFM has been used to characterize the inactivated viral particles of the SARS-CoV-2 strain, as well as the maturation and release phase of SARS-CoV virions from infected cells [100].

AFM can also be used to identify inactive virus particles [101, 102]. In addition to particle size selection, the nanomechanical properties of such particles have been investigated. For example, additional information about the viscoelastic properties and the Young's modulus of the particles may allow them to be identified and provide further information about their behavior in the presence of the host cell membrane [103].

Although AFM can be used to study viruses and virus-like particles, research on vaccine strains of poliovirus is underrepresented in the literature. AFM has been used to study the Sabin type I poliovirus vaccine strain Lse2ab [104]. It was demonstrated that such pseudoviral particle could be successfully adsorbed on a variety of surfaces, including titanium oxide, gold and palladium alloys, freshly cut mica, and graphite. Since the scanning was performed in the contact mode in air under these conditions, significant salt accumulation was observed. The diameters of the same particles were found

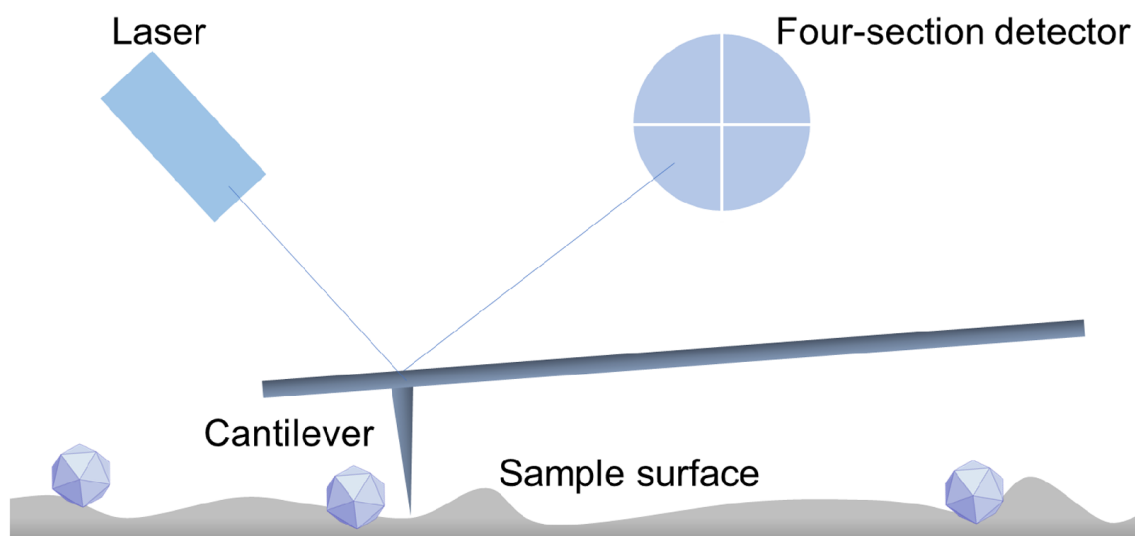


**Figure 13.** Principle of AFM. Physical forces between the probe and the virus particle cause cantilever deflection. The laser beam is directed to the outer surface of the cantilever, reflected and then falls on the four-section photodetector where it is converted into image information of the virus particle surface.

in another study using identical samples [105]. Their height was 29 nm. The difficulty of working with these objects and the small number of publications are probably due to the relatively small size of the objects studied and the high salt load of the initial samples.

Applied to poliovirus pseudoviral particles, AFM is applicable for quantitative and qualitative comparison of poliovirus particles inactivated by different methods, characterization of particle morphology and nanomechanical properties including the Young's modulus, and characterization of specific interaction with antibodies.

The AFM resolution is mainly determined by the radius of curvature of the probe. Two types of ultrasharp probes with different radius of curvature are used to analyze the fine structure: those with a silicon tip of  $\sim 2$  nm and those with blunter silicon nitride probes with carbon needles of  $\sim 1$  nm. The use of such probes will allow researchers to compare the fine structural spacing and protein packaging of viral particles inactivated in different ways.

It is reasonable to carry out the measurements in two different modes: tapping mode, in which the cantilever vibrations are generated at a resonant frequency, and PeakForce mode, in which the cantilever vibrations are excited at a nonresonant frequency and a force curve is recorded at each point in the image. It is useful to perform measurements not only in air but also in liquid to improve the image quality and bring it closer to native conditions.

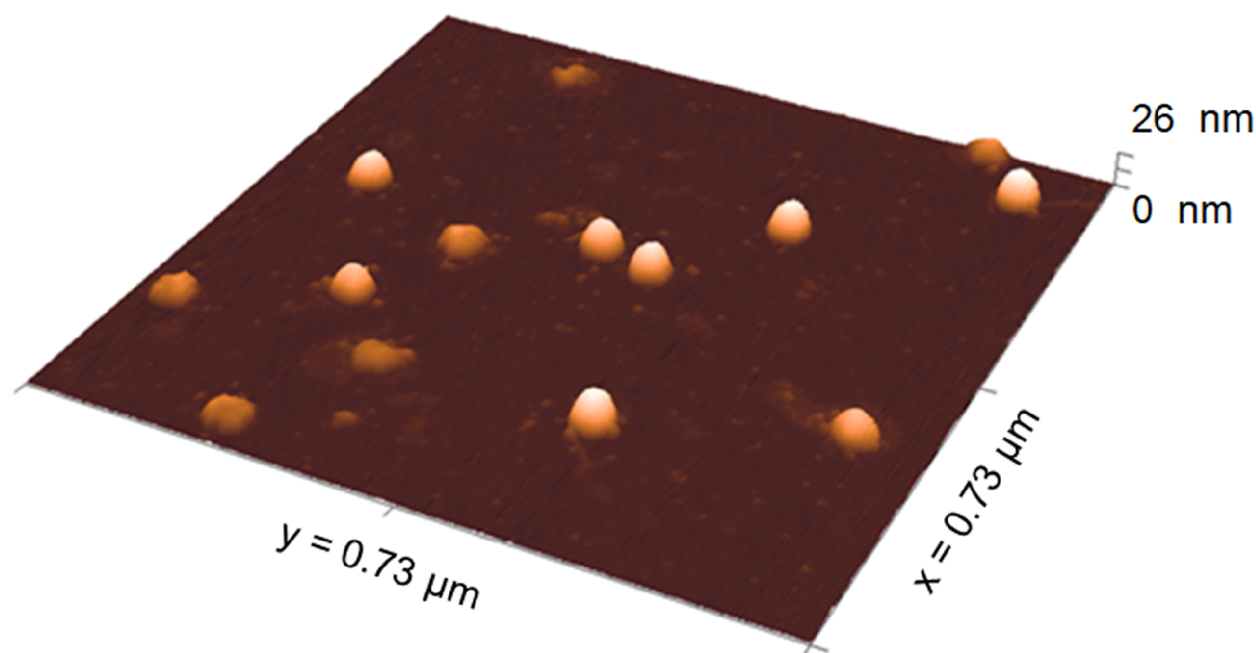
For example, a surface layer of water can be used to level the meniscus created between the cantilever and the substrate.

Figure 14 shows an AFM image of the Sabin II poliovirus vaccine strain.

#### 3.4. Analysis of the Interaction of the Viral Antigen (*D* antigen) with the Eukaryotic Cell Receptor (CD155) Using the Surface Plasmon Resonance-Based Method

Currently, surface plasmon resonance-based biosensors are widely used to study various interactions, including 1) protein-protein interaction [106, 107]; 2) antigen-antibody interaction [108]; 3) protein-lipid interaction [109, 110]; 4) low-molecular-weight ligand-protein interaction [111, 112]; and 5) the influence of low-molecular-weight compounds on protein-protein interactions [113, 114].

Surface plasmon resonance is a type of optical phenomenon that occurs when photon energy is transferred to electrons in a metal. The intensity of the reflected light decreases sharply at a certain angle of incidence (resonance angle) as the light energy is wasted in activating surface plasmons. The result is a damped light wave field. The resonance angle is determined by the refractive index of the medium in the surface layer. When a solution containing molecules that form complexes with molecules immobilized on the touch surface is injected, the refractive index of the surface layer changes, resulting in a change in the resonance angle. A complex formation curve [115] is used to record the change in resonance angle over time.



**Figure 14.** The AFM image of the Sabin II polio vaccine strain. The height of the particles is 26 nm. The AFM image was obtained in semicontact mode in air. The initial concentration of the suspension,  $\sim 10^7$  particles/ml, was applied to freshly cleaved mica, exposed for 5 min, washed with 1 ml of distilled water, and dried in a stream of nitrogen. The image was obtained at the Avogadro collaborative center at IBMC.

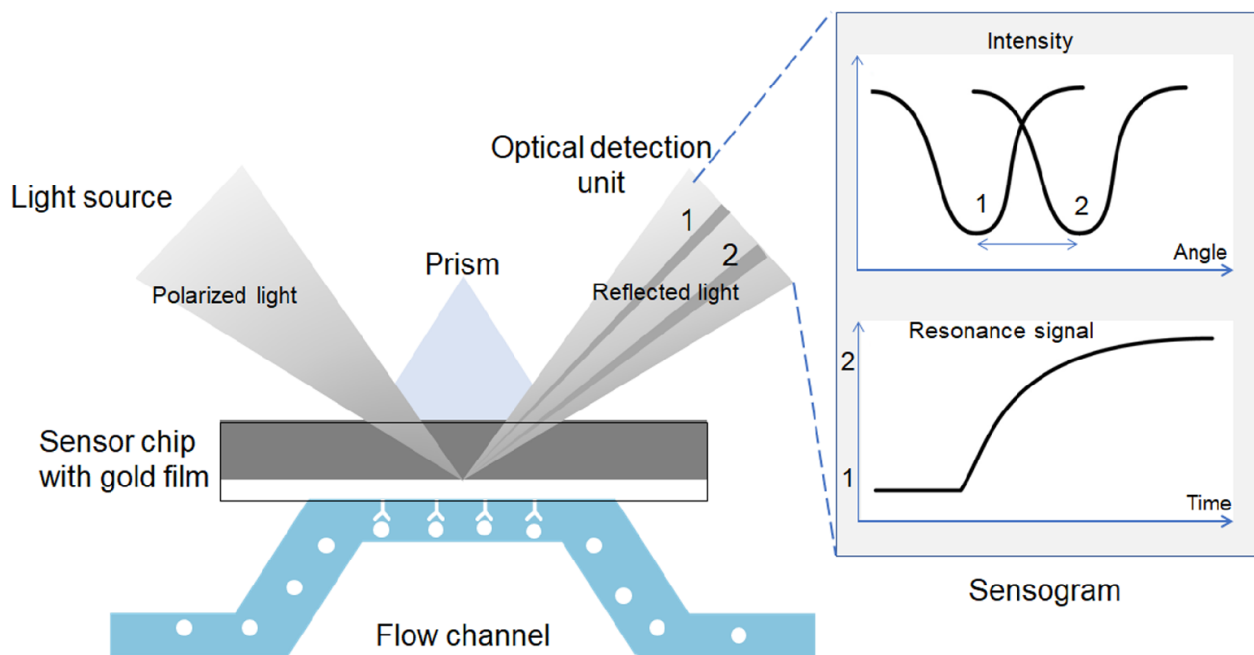


**Figure 15.** Principle of the SPR sensor work. Polarized light is reflected from a solution containing poliovirus particles. When a solution containing antibodies is introduced, complexes with the particles immobilized on the contact surface are formed, changing the refractive index in the surface layer and consequently the resonance angle. The change in the resonance angle over time is recorded as a complex formation curve (figure on the right).

The rate constants of association and dissociation, as well as the equilibrium dissociation constant, can be calculated by processing such curves obtained at different concentrations of the added analyte.

Surface plasmon resonance (SPR) biosensors (Fig. 15) have several significant advantages: a wide methodological range for oriented (His-tag, biotin) and nonoriented ( $-\text{SH}$ ,  $-\text{NH}_2$ ,  $-\text{COH}$ ) protein immobilization; the ability to study the interaction over a wide range of pH, ionic strength, temperature, flow rate and chemical composition of the working buffer; and the ability to regenerate a contact surface with immobilized protein under soft and hard conditions. Various substances, ranging from low molecular weight chemicals and peptides to whole cells and virus particles, can be used as analytes (molecules that interact with an immobilized molecule), and biosensors can be used in vaccine development and quality control [116].

A Biacore sensor based on surface plasmon resonance and monoclonal antibodies were used to assess the antigenicity of vaccines with or without adjuvant [117]. The Biacore sensor was also used to evaluate the stability of the hepatitis E vaccine [118]. In addition, determination of the binding affinity of cross-reactive antibodies to ACE2 and to S1-RBD using this sensor showed that the two monoclonal antibodies bound much weaker to ACE2 than to S1-RBD of the SARS-CoV-2 virus. This indicates that cross-reactive antibodies to ACE2 and to S1-RBD may be induced during SARS-CoV-2 infection due to potential antigenic cross-reactivity between

S1-RBD and its receptor (ACE2) [119]. In addition, SPR-based technology was used to screen inhibitors of virus entry and to study the interaction between immobilized HVEM (herpes virus entry mediator) and glycoprotein D in the presence of 8 different compounds. The compounds that decreased the biosensor signal level may serve as potential inhibitors of herpes virus entry into the cell [120].

Using the SPR technique, high-affinity monoclonal antibodies that efficiently neutralized both pseudotyped and live MERS-CoV strains were found. The significant neutralizing activity of these antibodies indicates their capability to prevent and treat MERS-CoV, as well as to be a tool for vaccine development [121]. Most research in the field of SPR technologies focuses on the interaction of antibodies with viral antigens [122–124]. The Biacore sensor has also been used to study the interactions of two animal viruses (vaccinia virus and poliovirus) and two plant viruses (cowpea mosaic virus and tobacco mosaic virus) with monoclonal antibodies in real time and in a label-free mode. Using monoclonal antibodies specific for different conformational states of the viral protein, it was found that viral particles (cowpea mosaic virus and tobacco mosaic virus) retained their structural integrity when immobilized on the dextran of the sensor chip [125].

Westdijk et al. quantified the D antigen using a SPR-based technique [126]. Since this technique does not require use of labels, incubation times or washing procedures, such assay reduces number of assay variations. Quantitative determination of the D antigen

in inactivated poliovirus samples can be performed using either a standard protocol with calibration curves for each serotype or the calibration-free concentration analysis (CFCA) format.

In the latter case, the analysis is based on the measurement of the binding rate during sample injection under conditions of partial or complete mass transfer limitation. The advantage of CFCA is that the technology does not require a calibration curve. By processing the sensorgrams, it is possible to obtain data describing the interaction of poliovirus with antibodies from the dependence of the biosensor signal on concentration: association rate constant, dissociation rate constant, and equilibrium dissociation constant. Thus, SPR-based biosensors are widely used in studies aimed at antigen-antibody and antibody-virus interactions [127].

### 3.5. Electrochemical Analysis of Surface Antigenic Proteins and Pseudoviral RNA

Electrochemical approaches in biochemical and medical research are rapidly developed due to advances in nanotechnology, nanomaterials, and algorithms for acquiring and processing electroanalytical results. Electrochemical analysis is based on the ability to record the processes that occur when biological molecules gain or release electrons. The advantages of electrochemical methods include real-time registration of all processes on the surface of the electrode, a small volume of the analyzed biological object (a few microliters), the ability to use both stationary and portable electrochemical devices with software and interchangeable electrodes, and the ability to obtain strictly reproducible results.

The type and modification of the electrode to immobilize the biomolecule and obtain an analytical signal is critical for an efficient electrochemical process associated with electron transfer. The advantage of using interchangeable electrodes is that they can be modified to optimize the electrochemical system, allowing the sensor to be adapted to the biological object or biomolecule being analyzed and providing the necessary analytical characteristics of the method, such as biocompatibility, detection limit, and range of determined concentrations.

Electrochemical devices for the detection of respiratory viruses have been developed based on genosensor and immunosensor techniques [128]. Data obtained using several methods for virus detection by RNA or viral proteins or antibodies have been summarized in [129–131]. Genosensors with immobilized DNA/RNA probes as recognition elements are applicable for the analysis of specific hybridization reactions by molecular recognition of DNA-DNA or DNA-RNA complexes [132–135]. The main advantages of these devices are their miniaturization potential, high sensitivity, low limits of detection (LOD) and the availability of software

for data processing. Based on the type of probe immobilization, i.e., the oligonucleotide to which the diagnosed genomic DNA or RNA sequence of the virus is attached, electrochemical genosensors are classified into three main categories:

- physical adsorption [135, 136] on the surface of the working electrode due to van der Waals interactions;
- chemical immobilization through the formation of covalent bonds [137–139] and bifunctional cross-linking with special reagents [140–142];
- rational design of sensor structures and recording circuits using various modifications of electrodes to enhance the signal [143, 144].

The conditions, under which the probe is immobilized, are important for the genosensor efficiency. The immobilization density of the oligonucleotide probe is proportional to the accessibility of the analyte binding sites. Excessive probe density can lead to sensor surface saturation and steric interference, which significantly decreases the hybridization efficiency [145–147]. Manzano et al. developed a genosensor based on thiol-Au interactions for the sensitive detection of hepatitis A virus cDNA. Changes in the oxidative potential of the indicator tripropylamine were observed after hybridization with the target due to inhibition of the effects of charge transfer and diffusion. The device achieved a limit of detection (LOD) of 6.94 fg/ $\mu$ l for viral cDNA, which was equal to the value obtained by PCR (6.4 fg/ $\mu$ l) [148].

Carinelli et al. used avidin-biotin interactions for efficient quantification of Ebola virus cDNA [149]. Ebola virus cDNA has been amplified using rolling-circle amplification (RCA) on magnetic beads (a step in which circularized biotinylated cDNA is bound to streptavidin-modified magnetic beads). Reamplification was performed by circular amplification (C2CA), and the products were detected by a double-labeling method using a biotinylated capture probe for immobilization on magnetic particles and a readout probe for electrochemical detection. Electrochemical detection was performed on printed graphite electrodes using H<sub>2</sub>O<sub>2</sub> reduction square wave voltammetry.

The electrochemical genosensor was able to detect 200 yoctamol ( $200 \times 10^{-24}$  mol) of cDNA, corresponding to 120 molecules of Ebola virus L-gene cDNA with a detection limit of 33 cDNA molecules. The LOD achieved with the strategy developed by the authors potentially allows early detection of the disease ( $10^6$  to  $10^{10}$  RNA copies/ml).

Streptavidin-biotin complexes were used to detect Ebola virus DNA on a gold-coated printed graphite electrode using differential pulse voltammetry (DIVA) [150]. Immobilized thiolated DNA was hybridized to the biotinylated target DNA strand on the electrode surface. A streptavidin-alkaline phosphatase conjugate was used to label the biotinylated

hybrid. The complementary oligonucleotides had a detection limit of 4.7 nM. An electrochemical readout of Ebola virus particles has been described in [151]. Ebola virus cDNA was amplified on magnetic beads and labeled with the glucose oxidase. The indirect electrochemical detection of target DNA is enabled by the enzymatic catalysis of glucose coupled to glucose oxidase.

Chronoamperometric determination of target DNA was performed using a Prussian blue-modified hydrogen peroxide monitoring electrode after glucose peroxidase administration. The methodology proposed in this paper allowed the determination of Ebola virus cDNA with an accuracy of 1.0 pmol/L (approximately  $6 \times 10^8$  target DNA/ml).

Streptavidin-biotin complexes have been used in works devoted to the electrochemical analysis of DNA of Zika virus [152] and (HPV)-16/18 [153] using horseradish peroxidase as a label. The detection limits of DNA by chronoamperometry were 0.7 pM and 0.1 ng for Zika virus and (HPV)-16/18, respectively.

Farzin et al. [147] developed an electrochemical device modified with amine functionalized ionic liquid and reduced graphene oxide for the detection of human papillomavirus (HPV)-16 cDNA. The material was applied to multiwalled carbon nanotube-modified electrodes and used to covalently bind aminated DNA probes using glutaraldehyde. In the presence of the sodium salt of anthraquinone-2-sulfonic acid monohydrate as an oxidatively active DNA intercalator, hybridization of ssDNA probes with target DNA strands of (HPV)-16 resulted in a significant increase in the response of the genosensor. The signal was measured by differential pulse voltammetry. The LOD for (HPV)-16 cDNA was 1.3 nM. Other proposed multilayer genosensors are based on a toluidine blue label for the detection of *Haemophilus influenzae* [139] and on the mediator ferrocene for hepatitis B detection [154].

The authors of [155] presented a 3D microfluidic analyzer based on graphene-modified paper electrodes as an alternative platform for hepatitis B analysis. Pyrrolidinyl peptide nucleic acid was covalently immobilized on a modified cellulose working electrode to capture target DNA due to its high affinity and selectivity for hepatitis B virus DNA. Depending on the concentration of hepatitis B virus DNA, the DIVA electrochemical signal of hexacyanoferrate (III)/(II) decreased in the presence of viral DNA. The limit of detection was 1.45 pM.

Electrochemical immunosensors work by converting immunochemical reaction information into a quantifiable signal that is proportional to the concentration of the analyte. This allows the sensors to identify different types of viruses. Sensor devices use an antibody or antigen, often immobilized on the sensor surface, as the biorecognition element [156].

The rapid response, high sensitivity, specificity, affordability, ease in use, and miniaturization are the features of electrochemical immunosensors that made them suitable for the diagnosis of viral infections. Numerous electrochemical immunosensors, including voltammetric, amperometric, impedimetric, and potentiometric, have been developed for virus detection. Electrochemical labels, electroactive mediators (ferrocene and ferricyanide), and enzymatic labels are used to record the electrochemical signal. Such immunosensors have been widely used to detect various types of viruses, including hepatitis B [157–163] and C [164–167], influenza viruses [168–172], Dengue [173–175], Zika [176], Japanese encephalitis [177, 178], measles [179], Newcastle disease virus [180], and enterovirus [181]. These types of sensors are considered to be a complementary approach to traditional quantitative RT-PCR.

Viral antigens are glycoproteins found on the surface of viruses that are responsible for binding to host cell receptors. For example, coronavirus entry into the host cell is mediated by the coronavirus envelope S protein [182], which was recently used as an antigen in an immunosensor for the diagnosis of COVID-19 [183]. An electroanalysis based on the detection of viral RNA or viral antigens (S protein) with high sensitivity has been developed for the diagnosis of COVID-19 [184, 185].

However, there is no description in the literature of a mediator-free (direct) electroanalysis of viral particle components based on the acquisition of electrochemical “signatures” (electrochemical profiling) of biomolecules during various biological processes. Previously, researchers at IBMC used electrochemical methods based on direct profiling of biological objects (transfected cells, DNA) to study cell transfection processes and to analyze DNA fragmentation under the influence of restriction enzymes and during apoptosis [186]. In studies on pseudoviral particle synthesis, electrochemical analysis methods were applied for comparative assessment of structural and biochemical properties (Fig. 16) after inactivation by ionizing radiation.

The efficiency of virus inactivation and production of pseudoviral particles depends on the degree of degradation of its genome [64]. Using analytical characteristics of voltammograms (potentials, maximum current amplitudes, areas under oxidation peaks) it is possible to obtain comparative profiles of poliovirus RNA oxidation based on the analysis of purine heterocyclic bases (guanine, adenine) and draw conclusions about the effect of the inactivation process on the integrity and fragmentation of viral RNA (left side of Figure 16).

A number of amino acids, such as tyrosine, tryptophan, histidine, methionine, and cysteine, have the unique property of undergoing electrochemical oxidation [187–189]. Since the preservation

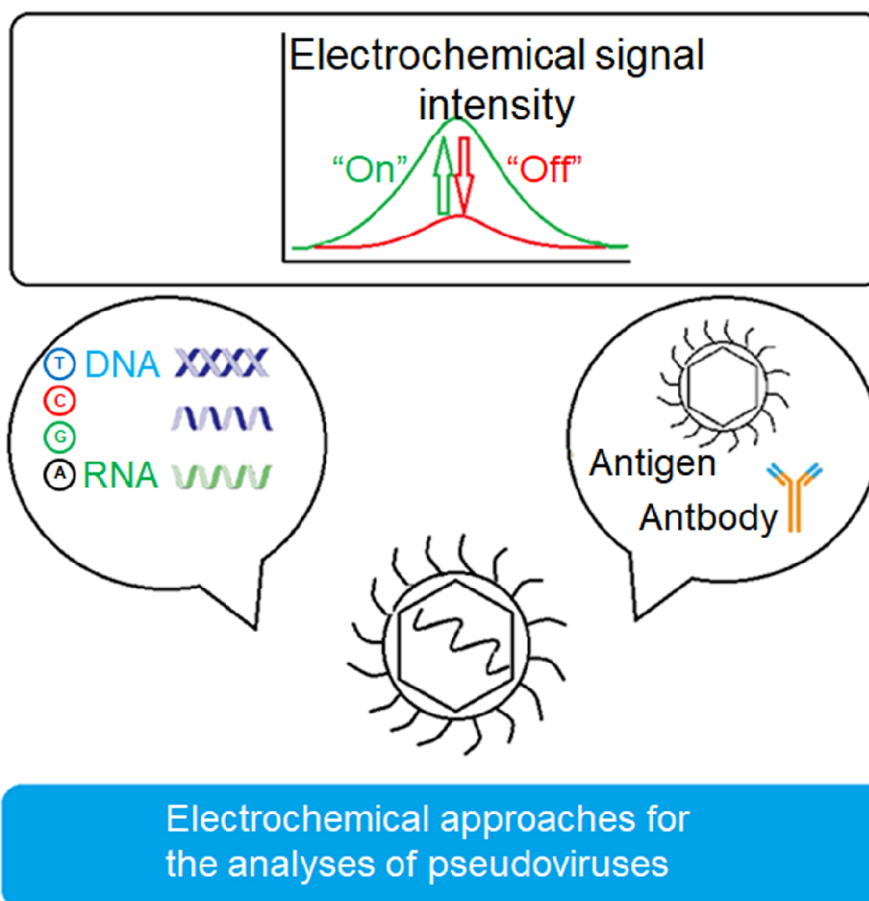


**Figure 16.** Electrochemical approaches to analyze the properties of components of pseudoviral particles. These include comparative profiling of surface antigenic proteins and nucleic acids of pseudoviruses to assess the influence of different inactivation parameters on the virus by changing the electrooxidation signal.

of the spatial structure of the D antigen is a problem that must be solved during the inactivation process [21], electrochemical profiling of D antigen viral proteins (right side of Figure 16) from different samples of poliovirus pseudoviral particles subjected to the inactivation process in different ways results in comparative profiles of viral proteins based on recording the electrochemical oxidation of amino acids in proteins of antigenic determinants to confirm the preservation of the spatial structure of the D antigen (Fig. 17).

The advantages of the electrochemical approach to protein detection are based on analysis of the processes of electrooxidation of amino acid residues: (1) direct detection at relatively low concentrations; (2) sensitivity to changes in protein conformation; and (3) signal change when amino acids are modified by electroactive groups.

Analysis of the components of pseudoviral particles (RNA, proteins) obtained by chemical inactivation and electron irradiation will help to study the comparative influence of chemical reagents and electron irradiation parameters on the electrochemical profile of polioviruses, reflecting the degree of damage to RNA and capsid proteins (VP1, VP2, VP3).

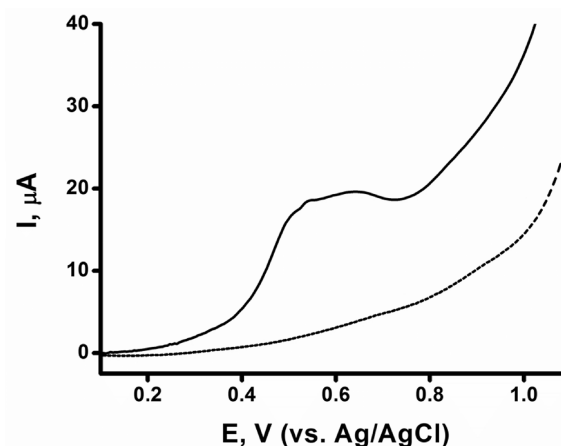


**Figure 17.** Square wave voltammograms in the absence of poliovirus (PGE/CNT, dotted curve) and in the presence of  $\beta$ -propiolactone-inactivated poliovirus, Sabin strain type 1 (PGE/CNT/poliovirus, black curve).

A comparative analysis of completely inactivated virus particles, which do not induce antibody formation and have a damaged or destroyed D antigen, and virus particles subjected to chemical inactivation and different doses of electron irradiation is among our future plans.

## CONCLUSIONS

The field of pseudoviral vaccines is becoming increasingly promising, but it is accompanied by tighter restrictions and the development of inactivation technologies as the process of developing a vaccine product accelerates. The most promising strategy appears to be the generation of pseudoviral vaccines using electron irradiation. The choice of dose and irradiation conditions makes it possible to induce changes in the virus genome that limit its replication capacity but preserve its immunogenic properties. Engineers and researchers can now design antiviral vaccines with ideal physicochemical properties, due to recent achievements in the theoretical and instrumental characteristics in the field of viruses and inactivated viral particles. The algorithms proposed and considered in this review, are adapted to characterization of poliovirus particles; they are a part of a platform for the development of pseudoviral vaccine preparations. The application of the platform algorithms will enable the development of promising new types of vaccines based on pseudoviral particles.

## FUNDING

The study was supported by the Russian Science Foundation grant No. 23-15-00471.

## COMPLIANCE WITH ETHICAL STANDARDS

This article does not contain any research involving humans or using animals as subjects.

## CONFLICT OF INTEREST

The authors declare no conflicts of interest.

## REFERENCES

- Hufsky F., Lamkiewicz K., Almeida A., Aouacheria A., Arighi C., Bateman A., Baumbach J., Beerenwinkel N., Brandt C., Cacciabue M., Chuguransky S., Drechsel O., Finn R.D., Fritz A., Fuchs S., Hattab G., Hauschild A.-C., Heider D., Hoffmann M., Hölzer M., Hoops S., Kaderali L., Kalvari I., von Kleist M., Kmiecinski R., Kühnert D., Lasso G., Libin P., List M., Löchel H.F., Martin M.J., Martin R., Matschinske J., McHardy A.C., Mendes P., Mistry J., Navratil V., Nawrocki E.P., O'Toole A.N., Ontiveros-Palacios N., Petrov A.I., Rangel-Pineros G., Redaschi N., Reimering S., Reinert K., Reyes A., Richardson L., Robertson D.L., Sadegh S., Singer J.B., Theys K., Upton C., Welzel M., Williams L., Marz M. (2021) Computational strategies to combat COVID-19: Useful tools to accelerate SARS-CoV-2 and coronavirus research. *Brief. Bioinform.*, **22**(2), 642-663. DOI: 10.1093/bib/bbaa232
- Fougeroux C., Goksøyr L., Idorn M., Soroka V., Myeni S.K., Dagil R., Janitzek C.M., Sogaard M., Aves K.-L., Horsted E.W., Erdoğan S.M., Gustavsson T., Dorosz J., Clemmensen S., Fredsgaard L., Thrane S., Vidal-Calvo E.E., Khalifé P., Hulen T.M., Choudhary S., Theisen M., Singh S.K., Garcia-Senosiaín A., van Oosten L., Pijlman G., Hierzberger B., Domeyer T., Nalewajek B.W., Strobæk A., Skrzypczak M., Andersson L.F., Buus S., Buus A.S., Christensen J.P., Dalebout T.J., Iversen K., Harritshoj L.H., Mordmuller B., Ullum H., Reinert L.S., de Jongh W.A., Kikkert M., Paludan S.R., Theander T.G., Nielsen M.A., Salanti A., Sander A.F. (2021) Capsid-like particles decorated with the SARS-CoV-2 receptor-binding domain elicit strong virus neutralization activity. *Nat. Commun.*, **12**(1), 324. DOI: 10.1038/s41467-020-20251-8
- Dong Y., Dai T., Wei Y., Zhang L., Zheng M., Zhou F. (2020) A systematic review of SARS-CoV-2 vaccine candidates. *Signal Transduct. Target. Ther.*, **5**(1), 237. DOI: 10.1038/s41392-020-00352-y
- Zhang B., Chao C.W., Tsybovsky Y., Abiona O.M., Hutchinson G.B., Moliva J.I., Olin A.S., Pegu A., Phung E., Stewart-Jones G.B.E., Verardi R., Wang L., Wang S., Werner A., Yang E.S., Yap C., Zhou T., Mascola J.R., Sullivan N.J., Graham B.S., Corbett K.S., Kwong P.D. (2020) A platform incorporating trimeric antigens into self-assembling nanoparticles reveals SARS-CoV-2-spike nanoparticles to elicit substantially higher neutralizing responses than spike alone. *Sci. Rep.*, **10**(1), 18149. DOI: 10.1038/s41598-020-74949-2
- Chen M., Zhang X.-E. (2021) Construction and applications of SARS-CoV-2 pseudoviruses: A mini review. *Int. J. Biol. Sci.*, **17**(6), 1574-1580. DOI: 10.7150/ijbs.59184
- Geng Q., Tai W., Baxter V.K., Shi J., Wan Y., Zhang X., Montgomery S.A., Taft-Benz S.A., Anderson E.J., Knight A.C., Dinno K.H., Leist S.R., Baric R.S., Shang J., Hong S.-W., Drelich A., Tseng C.-T.K., Jenkins M., Heise M., Du L., Li F. (2021) Novel virus-like nanoparticle vaccine effectively protects animal model from SARS-CoV-2 infection. *PLOS Pathog.*, **17**(9), e1009897. DOI: 10.1371/journal.ppat.1009897
- Xiang Q., Li L., Wu J., Tian M., Fu Y. (2022) Application of pseudovirus system in the development of vaccine, antiviral-drugs, and neutralizing antibodies. *Microbiol. Res.*, **258**, 126993. DOI: 10.1016/j.micres.2022.126993
- Jiang S.D., Pye D., Cox J.C. (1986) Inactivation of poliovirus with  $\beta$ -propiolactone. *J. Biol. Stand.*, **14**(2), 103-109. DOI: 10.1016/0092-1157(86)90028-4
- Wilton T., Dunn G., Eastwood D., Minor P.D., Martin J. (2014) Effect of formaldehyde inactivation on poliovirus. *J. Virol.*, **88**(20), 11955-11964. DOI: 10.1128/JVI.01809-14
- Fan C., Ye X., Ku Z., Kong L., Liu Q., Xu C., Cong Y., Huang Z. (2017) Beta-propiolactone inactivation of coxsackievirus A16 induces structural alteration and surface modification of viral capsids. *J. Virol.*, **91**(8), e00038-17. DOI: 10.1128/JVI.00038-17
- Fertey J., Thoma M., Beckmann J., Bayer L., Finkensieper J., Reißhauer S., Berneck B.S., Issmail L., Schönfelder J., Casado J.P., Poremba A., Rögner F.-H., Standfest B., Makert G.R., Walcher L., Kistenmacher A.-K., Fricke S., Grunwald T., Ulbert S. (2020) Automated application of low energy electron irradiation enables inactivation of pathogen- and cell-containing liquids in biomedical research and production facilities. *Sci. Rep.*, **10**(1), 12786. DOI: 10.1038/s41598-020-69347-7

12. *Avanzino B.C., Jue H., Miller C.M., Cheung E., Fuchs G., Fraser C.S.* (2018) Molecular mechanism of poliovirus Sabin vaccine strain attenuation. *J. Biol. Chem.*, **293**(40), 15471-15482. DOI: 10.1074/jbc.RA118.004913
13. *Bandyopadhyay A.S., Garon J., Seib K., Orenstein W.A.* (2015) Polio vaccination: Past, present and future. *Future Microbiol.*, **10**(5), 791-808. DOI: 10.2217/fmb.15.19
14. *Quarleri J.* (2023) Poliomyelitis is a current challenge: Long-term sequelae and circulating vaccine-derived poliovirus. *GeroScience*, **45**(2), 707-717. DOI: 10.1007/s11357-022-00672-7
15. *Klapsa D., Wilton T., Zealand A., Bujaki E., Saxentoff E., Troman C., Shaw A.G., Tedcastle A., Majumdar M., Mate R., Akello J.O., Huseynov S., Zeb A., Zambon M., Bell A., Hagan J., Wade M.J., Ramsay M., Grassly N.C., Saliba V., Martin J.* (2022) Sustained detection of type 2 poliovirus in London sewage between February and July, 2022, by enhanced environmental surveillance. *Lancet*, **400**, 1531-1538. DOI: 10.1016/S0140-6736(22)01804-9
16. *Okemoto-Nakamura Y., Someya K., Yamaji T., Saito K., Takeda M., Hanada K.* (2021) Poliovirus-nonsusceptible Vero cell line for the World Health Organization global action plan. *Sci. Rep.*, **11**(1), 6746. DOI: 10.1038/s41598-021-86050-3
17. *Bahar M.W., Porta C., Fox H., Macadam A.J., Fry E.E., Stuart D.I.* (2021) Mammalian expression of virus-like particles as a proof of principle for next generation polio vaccines. *NPJ vaccines*, **6**(1), 1-10. DOI: 10.1038/s41541-020-00267-3
18. *Hogle J.M.* (2002) Poliovirus cell entry: Common structural themes in viral cell entry pathways. *Annu. Rev. Microbiol.*, **56**(1), 677-702. DOI: 10.1146/annurev.micro.56.012302.160757
19. *Lentz K.N., Smith A.D., Geisler S.C., Cox S., Buontempo P., Skelton A., deMartino J., Rozhon E., Schwartz J., Girijavallabhan V., O'Connell J., Arnold E.* (1997) Structure of poliovirus type 2 Lansing complexed with antiviral agent SCH48973: Comparison of the structural and biological properties of the three poliovirus serotypes. *Structure*, **5**(7), 961-978. DOI: 10.1016/S0969-2126(97)00249-9
20. *He Y., Mueller S., Chipman P.R., Bator C.M., Peng X., Bowman V.D., Mukhopadhyay S., Wimmer E., Kuhn R.J., Rossmann M.G.* (2003) Complexes of poliovirus serotypes with their common cellular receptor, CD155. *J. Virol.*, **77**(8), 4827-4835. DOI: 10.1128/JVI.77.8.4827-4835.2003
21. *Karunatilaka K.S., Filman D.J., Strauss M., Loparo J.J., Hogle J.M.* (2021) Real-time imaging of polioviral RNA translocation across a membrane. *MBio*, **12**(1), e03695-20. DOI: 10.1128/mBio.03695-20
22. *Lashkevich V.A.* (2013) History of development of the live poliomyelitis vaccine from Sabin attenuated strains in 1959 and idea of poliomyelitis eradication. *Problems of Virology*, **58**(1), 4-10.
23. *Piniaeva A., Ignatyev G., Kozlovskaya L., Ivin Y., Kovpak A., Ivanov A., Shishova A., Antonova L., Khapchaev Y., Feldblum I., Ivanova O., Siniugina A., Ishmukhametov A.* (2021) Immunogenicity and safety of inactivated Sabin-strain polio vaccine "PoliovacSin": Clinical trials phase I and II. *Vaccines*, **9**(6), 565. DOI: 10.3390/vaccines9060565
24. *Ivanov A.P., Klebleyeva T.D., Ivanova O.E., Ipatova E.G., Gmyl L.V., Ishmukhametov A.A.* (2016) Experimental approaches to the development of inactivated poliovirus vaccine based on Sabin strains. *Epidemiol. Vaccine Prev.*, **15**(4), 59-64. DOI: 10.31631/2073-3046-2016-15-4-59-64
25. *Ivanov A.P., Klebleyeva T.D., Malyschkina L.P., Ivanova O.E.* (2019) Poliovirus-binding inhibition ELISA based on specific chicken egg yolk antibodies as an alternative to the neutralization test. *J. Virol. Methods*, **266**, 7-10. DOI: 10.1016/j.jviromet.2019.01.007
26. *Patterson E.I., Prince T., Anderson E.R., Casas-Sanchez A., Smith S.L., Cansado-Utrilla C., Solomon T., Griffiths M.J., Acosta-Serrano A., Turtle L., Hughes G.L.* (2020) Methods of inactivation of SARS-CoV-2 for downstream biological assays. *J. Infect. Dis.*, **222**(9), 1462-1467. DOI: 10.1093/infdis/jiaa507
27. *Auerswald H., Yann S., Dul S., In S., Dussart P., Martin N.J., Karlsson E.A., Garcia-Rivera J.A.* (2021) Assessment of inactivation procedures for SARS-CoV-2. *J. Gen. Virol.*, **102**(3), 001539. DOI: 10.1099/jgv.0.001539
28. *Delrue I., Verzele D., Madder A., Nauwynck H.J.* (2012) Inactivated virus vaccines from chemistry to prophylaxis: Merits, risks and challenges. *Expert Rev. Vaccines*, **11**(6), 695-719. DOI: 10.1586/erv.12.38
29. *Zhou S.S.* (2022) Variability and Relative Order of Susceptibility of Non-Enveloped Viruses to Chemical Inactivation. In: *Disinfection of Viruses* (Nims W.R., Ljaz M.K., eds.), Intechopen, 184 p. DOI: 10.5772/intechopen.102727
30. *Wigginton K.R., Pecsos B.M., Sigstam T., Bosshard F., Kohn T.* (2012) Virus inactivation mechanisms: Impact of disinfectants on virus function and structural integrity. *Environ. Sci. Technol.*, **46**(21), 12069-12078. DOI: 10.1021/es3029473
31. *Hossain F.* (2022) Sources, enumerations and inactivation mechanisms of four emerging viruses in aqueous phase. *J. Water Health*, **20**(2), 396-440. DOI: 10.2166/wh.2022.263
32. *Salthammer T., Mentese S., Marutzky R.* (2010) Formaldehyde in the indoor environment. *Chem. Rev.*, **110**(4), 2536-2572. DOI: 10.1021/cr800399g
33. *Sabbaghi A., Miri S.M., Keshavarz M., Zargar M., Ghaemi A.* (2019) Inactivation methods for whole influenza vaccine production. *Rev. Med. Virol.*, **29**(6), e2074. DOI: 10.1002/rmv.2074
34. *Kamps J.J.A.G., Hopkinson R.J., Schofield C.J., Claridge T.D.W.* (2019) How formaldehyde reacts with amino acids. *Commun. Chem.*, **2**(1), 126. DOI: 10.1038/s42004-019-0224-2
35. *Abd-Elghaffar A.A., Rashed M.E., Ali A.E., Amin M.A.* (2020) *In-vitro* inactivation of Sabin-polioviruses for development of safe and effective polio vaccine. *Vaccines*, **8**(4), 601. DOI: 10.3390/vaccines8040601
36. *Tobin G.J., Tobin J.K., Gaidamakova E.K., Wiggins T.J., Bushnell R. V., Lee W.-M., Matrosova V.Y., Dollery S.J., Meeks H.N., Kouivaskaia D., Chumakov K., Daly M.J.* (2020) A novel gamma radiation-inactivated Sabin-based polio vaccine. *PLoS One*, **15**(1), e0228006. DOI: 10.1371/journal.pone.0228006
37. *Kim E., Han G.-Y., Nguyen H.* (2017) An adenovirus-vectored influenza vaccine induces durable cross-protective hemagglutinin stalk antibody responses in mice. *Viruses*, **9**(8), 234. DOI: 10.3390/v9080234
38. *Fertey J., Bayer L., Grunwald T., Pohl A., Beckmann J., Gotzmann G., Casado J., Schonfelder J., Rogner F.-H., Wetzel C., Thoma M., Bailer S., Hiller E., Rupp S., Ulbert S.* (2016) Pathogens inactivated by low-energy-electron irradiation maintain antigenic properties and induce protective immune responses. *Viruses*, **8**(11), 319. DOI: 10.3390/v8110319

PERSPECTIVES FOR CREATING PSEUDOVIRUS-BASED VACCINES

39. Budowsky E., Friedman E., Zheleznova N., Noskov F. (1991) Principles of selective inactivation of viral genome. VI. Inactivation of the infectivity of the influenza virus by the action of  $\beta$ -propiolactone. *Vaccine*, **9**(6), 398-402. DOI: 10.1016/0264-410X(91)90125-P
40. Perrin P., Morgeaux S. (1995) Inactivation of DNA by  $\beta$ -propiolactone. *Biologicals*, **23**(3), 207-211. DOI: 10.1006/biol.1995.0034
41. Uittenbogaard J.P., Zomer B., Hoogerhout P., Metz B. (2011) Reactions of  $\beta$ -propiolactone with nucleobase analogues, nucleosides, and peptides. *J. Biol. Chem.*, **286**(42), 36198-36214. DOI: 10.1074/jbc.M111.279232
42. Herrera-Rodriguez J., Signorazzi A., Holtrop M., de Vries-Idema J., Huckriede A. (2019) Inactivated or damaged? Comparing the effect of inactivation methods on influenza virions to optimize vaccine production. *Vaccine*, **37**(12), 1630-1637. DOI: 10.1016/j.vaccine.2019.01.086
43. Yu S., Wei Y., Liang H., Ji W., Chang Z., Xie S., Wang Y., Li W., Liu Y., Wu H., Li J., Wang H., Yang X. (2022) Comparison of physical and biochemical characterizations of SARS-CoV-2 inactivated by different treatments. *Viruses*, **14**(9), 1938. DOI: 10.3390/v14091938
44. Savina N.N., Ekimov A.A., Trukhin V.P., Evtushenko A.E., Zhirenkina E.N., Sinegubova E.O., Slita A.V. (2021) Evaluation of avian adenovirus inactivation methods used in the production of influenza vaccines. *Extreme Medicine*, **3**, 78-83. DOI: 10.47183/mes.2021.032
45. Elveborg S., Monteil V., Mirazimi A. (2022) Methods of inactivation of highly pathogenic viruses for molecular, serology or vaccine development purposes. *Pathogens*, **11**(2), 271. DOI: 10.3390/pathogens11020271
46. Miller R.L., Plagemann P.G.W. (1974) Effect of ultraviolet light on mengovirus: Formation of uracil dimers, instability and degradation of capsid, and covalent linkage of protein to viral RNA. *J. Virol.*, **13**(3), 729-739. DOI: 10.1128/jvi.13.3.729-739.1974
47. Furuya Y., Regner M., Lobigs M., Koskinen A., Mullbacher A., Alsharifi M. (2010) Effect of inactivation method on the cross-protective immunity induced by whole "killed" influenza A viruses and commercial vaccine preparations. *J. Gen. Virol.*, **91**(6), 1450-1460. DOI: 10.1099/vir.0.018168-0
48. Grieb T., Forng R.-Y., Brown R., Owolabi T., Maddox E., Mcbain A., Drohan W.N., Mann D.M., Burgess W.H. (2002) Effective use of gamma irradiation for pathogen inactivation of monoclonal antibody preparations. *Biologicals*, **30**(3), 207-216. DOI: 10.1006/biol.2002.0330
49. Buenz E.J., Howe C.L. (2006) Picornaviruses and cell death. *Trends Microbiol.*, **14**(1), 28-36. DOI: 10.1016/j.tim.2005.11.003
50. Montagnon B.J., Nicolas A.J., Fanget B., Peyron L. (1981) Comparison of sensitivity of Vero cell line versus primary monkey kidney cells in the detection of residual live polio virus during and after inactivation. *Dev. Biol. Stand.*, **47**, 151-155.
51. Mendelsohn C.L., Wimmer E., Racaniello V.R. (1989) Cellular receptor for poliovirus: Molecular cloning, nucleotide sequence, and expression of a new member of the immunoglobulin superfamily. *Cell*, **56**(5), 855-865. DOI: 10.1016/0092-8674(89)90690-9
52. Chapel C., Rocher-Hélion N., Mantel N., Imbert S., Deshaies E., Barban V., Sabouraud A., Barbe J.-P., Mallet L. (2018) Replacement of primary monkey kidney cells by L20B cell line in the test for effective inactivation of inactivated poliovirus vaccine. *J. Virol. Methods*, **256**, 77-84. DOI: 10.1016/j.jviromet.2018.03.004
53. Kende M., Robbins M.L. (1965) Titration and neutralization of poliovirus in micro tissue culture under increased carbon dioxide. *Appl. Microbiol.*, **13**(6), 1026-1029. DOI: 10.1128/am.13.6.1026-1029.1965
54. Poliomyelitis vaccine (inactivated) version 9.2, 2010. Retrieved October 12, 2023, from <https://pdfsearches.com/european-pharmacopoeia-9-2>
55. Recommendations for the production and control of poliomyelitis vaccine (inactivated). Retrieved October 12, 2023, from [https://www.who.int/publications/m/item/recommendations-for-the-production-and-control-of-poliomyelitis-vaccine-\(inactivated\)](https://www.who.int/publications/m/item/recommendations-for-the-production-and-control-of-poliomyelitis-vaccine-(inactivated))
56. Beale A.J., Mason P.J. (1962) The measurement of the D-antigen in poliovirus preparations. *J. Hygiene (London)*, **60**(1), 113-121. DOI: 10.1017/S002217240003936X
57. Rezapkin G., Dragunsky E., Chumakov K. (2005) Improved ELISA test for determination of potency of inactivated poliovirus vaccine (IPV). *Biologicals*, **33**(1), 17-27. DOI: 10.1016/j.biologicals.2004.11.003
58. Ivanov A.P., Kozlov V.G., Klebleeva T.D., Ivanova O.E., Kiktenko A.V. (2014) An ELISA system based on the specific class Y (IgY) antibodies from egg yolks for the quantitative determination of D-antigen in inactivated poliovirus vaccines. *Problems of Virology*, **59**(6), 39-42.
59. Kouivaskaia D., Puligedda R.D., Dessain S.K., Chumakov K. (2020) Universal ELISA for quantification of D-antigen in inactivated poliovirus vaccines. *J. Virol. Methods*, **276**, 113785. DOI: 10.1016/j.jviromet.2019.113785
60. Wood D.J., Heath A.B., Sawyer L.A. (1995) A WHO collaborative study on assays of the antigenic content of inactivated poliovirus vaccines. *Biologicals*, **23**(1), 83-94. DOI: 10.1016/1045-1056(95)90017-9
61. Wilton T. (2016) Methods for the quality control of inactivated poliovirus vaccines. *Methods Mol. Biol.*, **1387**, 279-297. DOI: 10.1007/978-1-4939-3292-4\_15
62. Zhdanov D.D., Plyasova A.A., Pokrovsky V.S., Pokrovskaya M.V., Alexandrova S.S., Gladilina Y.A., Sokolov N.N. (2020) Inhibition of nuclease activity by a splice-switching oligonucleotide targeting deoxyribonuclease 1 mRNA prevents apoptosis progression and prolong viability of normal human CD4(+) T-lymphocytes. *Biochimie*, **174**, 34-43. DOI: 10.1016/j.biochi.2020.04.009
63. Zhdanov D.D., Gladilina Y.A., Pokrovsky V.S., Grishin D.V., Grachev V.A., Orlova V.S., Pokrovskaya M.V., Alexandrova S.S., Plyasova A.A., Sokolov N.N. (2019) Endonuclease G modulates the alternative splicing of deoxyribonuclease 1 mRNA in human CD4+ T lymphocytes and prevents the progression of apoptosis. *Biochimie*, **157**, 158-176. DOI: 10.1016/j.biochi.2018.11.020
64. Burton J., Love H., Richards K., Burton C., Summers S., Pitman J., Easterbrook L., Davies K., Spencer P., Killip M., Cane P., Bruce C., Roberts A.D.G. (2021) The effect of heat-treatment on SARS-CoV-2 viability and detection. *J. Virol. Methods*, **290**, 114087. DOI: 10.1016/j.jviromet.2021.114087
65. Baker M. (2011) qPCR: Quicker and easier but don't be sloppy. *Nat. Methods*, **8**(3), 207-212. DOI: 10.1038/nmeth0311-207
66. Holden M.J., Wang L. (2008) Quantitative Real-Time PCR: Fluorescent Probe Options and Issues. In: *Standardization and Quality Assurance in Fluorescence Measurements II* (Resch-Genger U., ed.). Springer Series on Fluorescence, vol. 6. Springer, Berlin, Heidelberg, pp. 489-508. DOI: 10.1007/4243\_2008\_046

67. Park H., Jung W., Jang H., Namkoong K., Choi K.-Y. (2022) One-step RT-qPCR for viral RNA detection using digital analysis. *Front. Bioeng. Biotechnol.*, **10**, 837838. DOI: 10.3389/fbioe.2022.837838
68. Wozniak A., Cerda A., Ibarra-Henriquez C., Sebastian V., Armijo G., Lamig L., Miranda C., Lagos M., Solari S., Guzmán A.M., Quiroga T., Hitschfeld S., Riveras E., Ferrés M., Gutiérrez R.A., García P. (2020) A simple RNA preparation method for SARS-CoV-2 detection by RT-qPCR. *Sci. Rep.*, **10**(1), 16608. DOI: 10.1038/s41598-020-73616-w
69. de Oliveira Lopes G.A., Ferreira L.R., de Souza Trindade G., Fonseca A.A., dos Reis J.K.P. (2021) qPCR assay for the detection of pseudocowpox virus. *Arch. Virol.*, **166**(1), 243-247. DOI: 10.1007/s00705-020-04872-4
70. Sabat J., Subhadra S., Rath S., Ho L.M., Kanungo S., Panda S., Mandal M.C., Dash S., Pati S., Turuk J. (2021) Yielding quality viral RNA by using two different chemistries: A comparative performance study. *Biotechniques*, **71**(4), 510-515. DOI: 10.2144/btn-2021-0054
71. Reichelt R. (2007) Scanning Electron Microscopy. In: *Science of Microscopy* (Hawkes P.W., Spence J.C.H., eds.), Springer, New York, NY, pp. 133-272. DOI: 10.1007/978-0-387-49762-4\_3
72. Singh A.K. (2016) Experimental Methodologies for the Characterization of Nanoparticles. In: *Engineered Nanoparticles*, Stanford University, pp. 125-170. DOI: 10.1016/B978-0-12-801406-6.00004-2
73. Ulery B.D., Kumar D., Ramer-Tait A.E., Metzger D.W., Wannemuehler M.J., Narasimhan B. (2011) Design of a protective single-dose intranasal nanoparticle-based vaccine platform for respiratory infectious diseases. *PLoS One*, **6**(3), e17642. DOI: 10.1371/journal.pone.0017642
74. Kipper M.J., Wilson J.H., Wannemuehler M.J., Narasimhan B. (2006) Single dose vaccine based on biodegradable polyanhydride microspheres can modulate immune response mechanism. *J. Biomed. Mater. Res. Part A*, **76A**(4), 798-810. DOI: 10.1002/jbm.a.30545
75. Ross K.A., Loyd H., Wu W., Huntimer L., Wannemuehler M.J., Carpenter S., Narasimhan B. (2014) Structural and antigenic stability of H5N1 hemagglutinin trimer upon release from polyanhydride nanoparticles. *J. Biomed. Mater. Res. Part A*, **102**(11), 4161-4168. DOI: 10.1002/jbm.a.35086
76. Ingvarsson P.T., Schmidt S.T., Christensen D., Larsen N.B., Hinrichs W.L.J., Andersen P., Rantanen J., Nielsen H.M., Yang M., Foged C. (2013) Designing CAF-adjuvanted dry powder vaccines: Spray drying preserves the adjuvant activity of CAF01. *J. Control. Release*, **167**(3), 256-264. DOI: 10.1016/j.jconrel.2013.01.031
77. Vangala A., Kirby D., Rosenkrands I., Agger E.M., Andersen P., Perrie Y. (2010) A comparative study of cationic liposome and niosome-based adjuvant systems for protein subunit vaccines: Characterisation, environmental scanning electron microscopy and immunisation studies in mice. *J. Pharm. Pharmacol.*, **58**(6), 787-799. DOI: 10.1211/jpp.58.6.0009
78. Lee J.T.Y., Chow K.L. (2012) SEM sample preparation for cells on 3D scaffolds by freeze-drying and HMDS. *Scanning*, **34**(1), 12-25. DOI: 10.1002/sca.20271
79. Williams D.B., Carter C.B. (2009) The Transmission Electron Microscope. In: *Transmission Electron Microscopy*. Springer, Boston, MA, pp. 3-22. DOI: 10.1007/978-0-387-76501-3\_1
80. Newbury D.E., Joy D.C., Echlin P., Fiori C.E., Goldstein J.I. (1986) Cryomicroscopy. In: *Advanced Scanning Electron Microscopy and X-Ray Microanalysis*. Springer, Boston, MA, pp. 365-433. DOI: 10.1007/978-1-4757-9027-6\_9
81. Callaway E. (2015) The revolution will not be crystallized: A new method sweeps through structural biology. *Nature*, **525**(7568), 172-174. DOI: 10.1038/525172a
82. Rames M., Yu Y., Ren G. (2014) Optimized negative staining: A high-throughput protocol for examining small and asymmetric protein structure by electron microscopy. *J. Vis. Exp.*, 2014(90), e51087. DOI: 10.3791/51087
83. Taylor A.R., McCormick M.J. (1956) Electron microscopy of poliomyelitis virus. *Yale J. Biol. Med.*, **28**(6), 589-597.
84. Dales S., Eggers H.J., Tamm I., Palade G.E. (1965) Electron microscopic study of the formation of poliovirus. *Virology*, **26**(3), 379-389. DOI: 10.1016/0042-6822(65)90001-2
85. Belnap D.M., McDermott B.M., Filman D.J., Cheng N., Trus B.L., Zuccola H.J., Racaniello V.R., Hogle J.M., Steven A.C. (2000) Three-dimensional structure of poliovirus receptor bound to poliovirus. *Proc. Natl. Acad. Sci.*, **97**(1), 73-78. DOI: 10.1073/pnas.97.1.73
86. Bubeck D., Filman D.J., Hogle J.M. (2005) Cryo-electron microscopy reconstruction of a poliovirus-receptor-membrane complex. *Nat. Struct. Mol. Biol.*, **12**(7), 615-618. DOI: 10.1038/nsmb955
87. Rossignol E., Yang J., Bullitt E. (2015) The role of electron microscopy in studying the continuum of changes in membranous structures during poliovirus infection. *Viruses*, **7**(10), 5305-5318. DOI: 10.3390/v7102874
88. Binnig G., Quate C.F., Gerber C. (1986) Atomic force microscope. *Phys. Rev. Lett.*, **56**(9), 930-933. DOI: 10.1103/PhysRevLett.56.930
89. Loh S., Cheah W. (2017) Optical beam deflection based AFM with integrated hardware and software platform for an undergraduate engineering laboratory. *Appl. Sci.*, **7**(3), 226. DOI: 10.3390/app7030226
90. Trent A., Ulery B.D., Black M.J., Barrett J.C., Liang S., Kostenko Y., David N.A., Tirrell M.V. (2015) Peptide amphiphile micelles self-adjuvant group A streptococcal vaccination. *AAPS J.*, **17**(2), 380-388. DOI: 10.1208/s12248-014-9707-3
91. Akhmetova A.I., Yaminsky I.V. (2022) High resolution imaging of viruses: Scanning probe microscopy and related techniques. *Methods*, **197**, 30-38. DOI: 10.1016/j.ymeth.2021.06.011
92. de Pablo P.J., Schaap I.A.T. (2019) Atomic force microscopy of viruses. *Phys. Virol. Adv. Exp. Med. Biol.*, **1215**, 159-179. DOI: 10.1007/978-3-030-14741-9\_8
93. Malkin A.J., Plomp M., McPherson A. (2005) Unraveling the architecture of viruses by high-resolution atomic force microscopy. *Methods Mol. Biol.*, **292**, 85-108. DOI: 10.1385/1-59259-848-X:085
94. Kuznetsov Y.G., Malkin A.J., Lucas R.W., Plomp M., McPherson A. (2001) Imaging of viruses by atomic force microscopy. *J. Gen. Virol.*, **82**(9), 2025-2034. DOI: 10.1099/0022-1317-82-9-2025
95. Liashkovich I., Hafezi W., Kuhn J.E., Oberleithner H., Kramer A., Shahin V. (2008) Exceptional mechanical and structural stability of HSV-1 unveiled with fluid atomic force microscopy. *J. Cell Sci.*, **121**(14), 2287-2292. DOI: 10.1242/jcs.032284
96. Sae-Ueng U., Li D., Zuo X., Huffman J.B., Homa F.L., Rau D., Evilevitch A. (2014) Solid-to-fluid DNA transition inside HSV-1 capsid close to the temperature of infection. *Nat. Chem. Biol.*, **10**(10), 861-867. DOI: 10.1038/nchembio.1628

97. Dubrovin E.V., Voloshin A.G., Kraevskiy S.V., Ignatyuk T.E., Abramchuk S.S., Yaminsky I.V., Ignatov S.G. (2008) Atomic force microscopy investigation of phage infection of bacteria. *Langmuir*, **24**(22), 13068-13074. DOI: 10.1021/la8022612
98. Dubrovin E.V., Popova A.V., Kraevskiy S.V., Ignatov S.G., Ignatyuk T.E., Yaminsky I.V., Volozhantsev N.V. (2012) Atomic force microscopy analysis of the *Acinetobacter baumannii* bacteriophage AP22 lytic cycle. *PLoS One*, **7**(10), e47348. DOI: 10.1371/journal.pone.0047348
99. Alsteens D., Newton R., Schubert R., Martinez-Martin D., Delguste M., Roska B., Müller D.J. (2017) Nanomechanical mapping of first binding steps of a virus to animal cells. *Nat. Nanotechnol.*, **12**(2), 177-183. DOI: 10.1038/nnano.2016.228
100. Bagrov D.V., Glukhov G.S., Moiseenko A.V., Karlova M.G., Litvinov D.S., Zaitsev P.A., Kozlovskaya L.I., Shishova A.A., Koypak A.A., Ivin Y.Y., Pinaeva A.N., Oksanich A.S., Volok V.P., Osolodkin D.I., Ishmukhametov A.A., Egorov A.M., Shaitan K.V., Kirpichnikov M.P., Sokolova O.S. (2022) Structural characterization of  $\beta$ -propiolactone inactivated severe acute respiratory syndrome coronavirus 2 (SARS-CoV-2) particles. *Microsc. Res. Tech.*, **85**(2), 562-569. DOI: 10.1002/jemt.23931
101. Nooraei S., Bahrulolulm H., Hoseini Z.S., Katalani C., Hajizade A., Easton A.J., Ahmadian G. (2021) Virus-like particles: Preparation, immunogenicity and their roles as nanovaccines and drug nanocarriers. *J. Nanobiotechnology*, **19**(1), 59. DOI: 10.1186/s12951-021-00806-7
102. Oropesa R., Ramos J.R., Falcón V., Felipe A. (2013) Characterization of virus-like particles by atomic force microscopy in ambient conditions. *Adv. Nat. Sci. Nanosci. Nanotechnol.*, **4**(2), 025007. DOI: 10.1088/2043-6262/4/2/025007
103. González-Domínguez I., Gutiérrez-Granados S., Cervera L., Gódia F., Domingo N. (2016) Identification of HIV-1-based virus-like particles by multifrequency atomic force microscopy. *Biophys. J.*, **111**(6), 1173-1179. DOI: 10.1016/j.bpj.2016.07.046
104. Yaminsky I.V., Bolshakova A.V., Loginov B.A., Protasenko V.V., Suvorov A.L., Kozodaev M.A., Volnin D.S. (2000) Microscopic control on content of poliomyelitis virus. *Surf. Investig. X-Ray, Synchrotron Neutron Tech.*, **15**, 1119-1125.
105. Golutvin I.A. (2004) Scanning force spectroscopy of nanostructured polymer and biological systems. *dis. Ph.D. physics and mathematics Sciences*, Federal State Unitary Enterprise State Scientific Center of the Russian Federation Institute of Theoretical and Experimental Physics, Moscow.
106. Yablokov E.O., Sushko T.A., Ershov P.V., Florinskaya A.V., Gnedenko O.V., Shkel T.V., Grabovec I.P., Strushkevich N.V., Kaluzhskiy L.A., Usanov S.A., Gilep A.A., Ivanov A.S. (2019) A large-scale comparative analysis of affinity, thermodynamics and functional characteristics of interactions of twelve cytochrome P450 isoforms and their redox partners. *Biochimie*, **162**, 156-166. DOI: 10.1016/j.biochi.2019.04.020.
107. Gnedenko O.V., Yablokov E.O., Ershov P.V., Svirid A.V., Shkel T.V., Haidukevich I.V., Strushkevich N.V., Gilep A.A., Usanov S.A., Ivanov A.S. (2019) Interaction of prostacyclin synthase with cytochromes P450. *Biomeditsinskaya Khimiya*, **65**(1), 63-66. DOI: 10.18097/PBMC20196501063
108. Gnedenko O.V., Mezentssev Y.V., Molnar A.A., Lisitsa A.V., Ivanov A.S., Archakov A.I. (2013) Highly sensitive detection of human cardiac myoglobin using a reverse sandwich immunoassay with a gold nanoparticle-enhanced surface plasmon resonance biosensor. *Anal. Chim. Acta*, **759**, 105-109. DOI: 10.1016/j.aca.2012.10.053.
109. Kaluzhskiy L.A., Ershov P.V., Kurpedinov K.S., Sonina D.S., Yablokov E.O., Shkel T.V., Haidukevich I.V., Sergeev G.V., Usanov S.A., Ivanov A.S. (2019) SPR analysis of protein-protein interactions with P450 cytochromes and cytochrome b5 integrated into lipid membrane. *Biomeditsinskaya Khimiya*, **65**(5), 374-379. DOI: 10.18097/PBMC20196505374
110. Ershov P.V., Kaluzhskiy L.A., Yablokov E.O., Gnedenko O.V., Kavaleuski A.A., Tumilovich A.M., Gilep A.A., Strushkevich N.V., Ivanov A.S. (2021) Application of the SPR biosensor for the analysis of protein-protein interactions in aqueous environment and bilayer lipid membrane as exemplified by P450sc (CYP11A1). *Biochemistry (Moscow), Suppl. Ser. A Membr. Cell Biol.*, **15**(1), 89-96. DOI: 10.1134/S1990747821010049
111. Kaluzhskiy L., Ershov P., Yablokov E., Shkel T., Grabovec I., Mezentssev Y., Gnedenko O., Usanov S., Shabunya P., Fatykhava S., Popov A., Artyukov A., Styshova O., Gilep A., Strushkevich N., Ivanov A. (2021) Human lanosterol 14-alpha demethylase (CYP51A1) is a putative target for natural flavonoid luteolin 7,3'-disulfate. *Molecules*, **26**(8), 2237. DOI: 10.3390/molecules26082237.
112. Kaluzhskiy L.A., Ershov P.V., Yablokov E.O., Mezentssev Y.V., Gnedenko O.V., Shkel T.V., Gilep A.A., Usanov S.A., Ivanov A.S. (2021) Screening of potential non-azole inhibitors of lanosterol 14-alpha demethylase (CYP51) of *Candida* fungi. *Biomeditsinskaya Khimiya*, **67**(1), 42-50. DOI: 10.18097/PBMC20216701042
113. Yablokov E.O., Sushko T.A., Kaluzhskiy L.A., Kavaleuski A.A., Mezentssev Y.V., Ershov P.V., Gilep A.A., Ivanov A.S., Strushkevich N.V. (2021) Substrate-induced modulation of protein-protein interactions within human mitochondrial cytochrome P450-dependent system. *J. Steroid Biochem. Mol. Biol.*, **208**, 105793. DOI: 10.1016/j.jsbmb.2020.105793
114. Ershov P.V., Yablokov E.O., Florinskaya A.V., Mezentssev Y.V., Kaluzhskiy L.A., Tumilovich A.M., Gilep A.A., Usanov S.A., Ivanov A.S. (2019) SPR-based study of affinity of cytochrome P450s / redox partners interactions modulated by steroidal substrates. *J. Steroid Biochem. Mol. Biol.*, **187**, 124-129. DOI: 10.1016/j.jsbmb.2018.11.009
115. van der Merwe P.A. (2001) Surface Plasmon Resonance. In: *Protein-Ligand Interactions: Hydrodynamics and Calorimetry* (Harding S.E., Chowdry B.Z., eds.), Oxford University Press, New York, pp. 137-170.
116. Ivanov A.S. (2012) The study of intermolecular interactions using optical biosensors operating on the effect of surface plasmon resonance. *Sovremennyye Tehnologii v Medicine*, **4**, 142-152.
117. Yin X., Wang X., Zhang Z., Li Y., Lin Z., Pan H., Gu Y., Li S., Zhang J., Xia N., Zhao Q. (2020) Demonstration of real-time and accelerated stability of hepatitis E vaccine with a combination of different physicochemical and immunochemical methods. *J. Pharm. Biomed. Anal.*, **177**, 112880. DOI: 10.1016/j.jpba.2019.112880
118. Li Y., Huang X., Zhang Z., Li S., Zhang J., Xia N., Zhao Q. (2020) Prophylactic hepatitis E vaccines: Antigenic analysis and serological evaluation. *Viruses*, **12**(1), 109. DOI: 10.3390/v12010109

119. Lai Y.-C., Cheng Y.-W., Chao C.-H., Chang Y.-Y., Chen C.-D., Tsai W.-J., Wang S., Lin Y.-S., Chang C.-P., Chuang W.-J., Chen L.-Y., Wang Y.-R., Chang S.-Y., Huang W., Wang J.-R., Tseng C.-K., Lin C.-K., Chuang Y.-C., Yeh T.-M. (2022) Antigenic cross-reactivity between SARS-CoV-2 S1-RBD and its receptor ACE2. *Front. Immunol.*, **13**, 868724. DOI: 10.3389/fimmu.2022.868724
120. Kumar P.K.R. (2020) Systematic screening of viral entry inhibitors using surface plasmon resonance. *Methods Mol. Biol.*, **2089**, 131-145. DOI: 10.1007/978-1-0716-0163-1\_8
121. Ying T., Du L., Ju T.W., Prabakaran P., Lau C.C.Y., Lu L., Liu Q., Wang L., Feng Y., Wang Y., Zheng B.-J., Yuen K.-Y., Jiang S., Dimitrov D.S. (2014) Exceptionally potent neutralization of middle east respiratory syndrome coronavirus by human monoclonal antibodies. *J. Virol.*, **88**(14), 7796-7805. DOI: 10.1128/JVI.00912-14
122. Rossi G., Real-Fernández F., Panza F., Barbetti F., Pratesi F., Rovero P., Migliorini P. (2014) Biosensor analysis of anti-citrullinated protein/peptide antibody affinity. *Anal. Biochem.*, **465**, 96-101. DOI: 10.1016/j.ab.2014.07.030
123. Okagawa T., Konnai S., Nishimori A., Maekawa N., Ikebuchi R., Goto S., Nakajima C., Kohara J., Ogasawara S., Kato Y., Suzuki Y., Murata S., Ohashi K. (2017) Anti-bovine programmed death-1 rat-bovine chimeric antibody for immunotherapy of bovine leukemia virus infection in cattle. *Front. Immunol.*, **8**, 650. DOI: 10.3389/fimmu.2017.00650
124. Wong C.L., Chua M., Mittman H., Choo L.X., Lim H.Q., Olivo M. (2017) A phase-intensity surface plasmon resonance biosensor for avian influenza A (H5N1) detection. *Sensors*, **17**(10), 2363. DOI: 10.3390/s17102363
125. Dubs M.-C., Altschuh D., van Regenmortel M.H.V. (1992) Interaction between viruses and monoclonal antibodies studied by surface plasmon resonance. *Immunol. Lett.*, **31**(1), 59-64. DOI: 10.1016/0165-2478(92)90011-C
126. Westdijk J., van der Maas L., ten Have R., Kersten G. (2016) Measuring poliovirus antigenicity by surface plasmon resonance. Application for potency indicating assays. *Methods Mol. Biol.*, **1387**, 299-323. DOI: 10.1007/978-1-4939-3292-4\_16
127. Visentin J., Minder L., Lee J.-H., Taupin J.-L., di Primo C. (2016) Calibration free concentration analysis by surface plasmon resonance in a capture mode. *Talanta*, **148**, 478-485. DOI: 10.1016/j.talanta.2015.11.025
128. Sobhanie E., Salehnia F., Xu G., Hamidipanah Y., Arshian S., Firoozbakhtian A., Hosseini M., Ganjali M.R., Hanif S. (2022) Recent trends and advancements in electrochemiluminescence biosensors for human virus detection. *Trends Anal. Chem.*, **157**, 116727. DOI: 10.1016/j.trac.2022.116727
129. Ribeiro B.V., Cordeiro T.A.R., Oliveira e Freitas G.R., Ferreira L.F., Franco D.L. (2020) Biosensors for the detection of respiratory viruses: A review. *Talanta Open*, **2**, 100007. DOI: 10.1016/j.talo.2020.100007
130. Traipop S., Jampasa S., Tangkijvanich P., Chuaypen N., Chailapakul O. (2023) Dual-label vertical flow-based electrochemical immunosensor for rapid and simultaneous detection of hepatitis B surface and e virus antigens. *Sensors Actuators B Chem.*, **387**, 133769. DOI: 10.1016/j.snb.2023.133769
131. Martins G., Gogola J.L., Budni L.H., Janegitz B.C., Marcolino-Junior L.H., Bergamini M.F. (2021) 3D-printed electrode as a new platform for electrochemical immunosensors for virus detection. *Anal. Chim. Acta*, **1147**, 30-37. DOI: 10.1016/j.aca.2020.12.014
132. Pividori M. (2000) Electrochemical genosensor design: Immobilisation of oligonucleotides onto transducer surfaces and detection methods. *Biosens. Bioelectron.*, **15**(5-6), 291-303. DOI: 10.1016/S0956-5663(00)00071-3
133. Rasheed P.A., Sandhyarani N. (2017) Carbon nanostructures as immobilization platform for DNA: A review on current progress in electrochemical DNA sensors. *Biosens. Bioelectron.*, **97**, 226-237. DOI: 10.1016/j.bios.2017.06.001
134. da Fonseca Alves R., Franco D.L., Cordeiro M.T., de Oliveira E.M., Fireman Dutra R.A., Sotomayor M.D.P.T. (2019) Novel electrochemical genosensor for Zika virus based on a poly-(3-amino-4-hydroxybenzoic acid)-modified pencil carbon graphite electrode. *Sensors Actuators B Chem.*, **296**, 126681. DOI: 10.1016/j.snb.2019.126681
135. Wang J., Cai X., Rivas G., Shirashi H., Dontha N. (1997) Nucleic-acid immobilization, recognition and detection at chronopotentiometric DNA chips. *Biosens. Bioelectron.*, **12**(7), 587-599. DOI: 10.1016/S0956-5663(96)00076-0
136. Erdem A., Pividori M.L., del Valle M., Alegret S. (2004) Rigid carbon composites: A new transducing material for label-free electrochemical genosensing. *J. Electroanal. Chem.*, **567**(1), 29-37. DOI: 10.1016/j.jelechem.2003.10.049
137. Zhang Y., Wang J., Xu M. (2010) A sensitive DNA biosensor fabricated with gold nanoparticles/poly(p-aminobenzoic acid)/carbon nanotubes modified electrode. *Colloids Surfaces B Biointerfaces*, **75**(1), 179-185. DOI: 10.1016/j.colsurfb.2009.08.030
138. Balasubramanian K., Burghard M. (2005) Chemically functionalized carbon nanotubes. *Small*, **1**(2), 180-192. DOI: 10.1002/smll.200400118
139. Saadati A., Hassanpour S., Hasanzadeh M., Shadjou N. (2020) Binding of pDNA with cDNA using hybridization strategy towards monitoring of *Haemophilus influenzae* genome in human plasma samples. *Int. J. Biol. Macromol.*, **150**, 218-227. DOI: 10.1016/j.ijbiomac.2020.02.062
140. Marrazza G., Chianella I., Mascini M. (1999) Disposable DNA electrochemical sensor for hybridization detection. *Biosens. Bioelectron.*, **14**(1), 43-51. DOI: 10.1016/S0956-5663(98)00102-X
141. Riccardi C.S., Dahmouche K., Santilli C.V., da Costa P.I., Yamanaka H. (2006) Immobilization of streptavidin in sol-gel films: Application on the diagnosis of hepatitis C virus. *Talanta*, **70**(3), 637-643. DOI: 10.1016/j.talanta.2006.01.027
142. Dong S., Zhao R., Zhu J., Lu X., Li Y., Qiu S., Jia L., Jiao X., Song S., Fan C., Hao R., Song H. (2015) Electrochemical DNA biosensor based on a tetrahedral nanostructure probe for the detection of avian influenza A (H7N9) virus. *ACS Appl. Mater. Interfaces*, **7**(16), 8834-8842. DOI: 10.1021/acsami.5b01438
143. Sajid M., Nazal M.K., Mansha M., Alsharaa A., Jillani S.M.S., Basheer C. (2016) Chemically modified electrodes for electrochemical detection of dopamine in the presence of uric acid and ascorbic acid: A review. *Trends Anal. Chem.*, **76**, 15-29. DOI: 10.1016/j.trac.2015.09.006
144. Shumyantseva V.V., Agafonova L.E., Bulko T.V., Kuzikov A.V., Masamrekh R.A., Yuan J., Pergushov D.V., Sigolaeva L.V. (2021) Electroanalysis of biomolecules: Rational selection of sensor construction. *Biochemistry (Moscow)*, **86**(S1), S140-S151. DOI: 10.1134/S0006297921140108
145. Movilli J., Rozzi A., Ricciardi R., Corradini R., Huskens J. (2018) Control of probe density at DNA biosensor surfaces using poly(L-lysine) with appended reactive groups. *Bioconjug. Chem.*, **29**(12), 4110-4118. DOI: 10.1021/acs.bioconjchem.8b00733

146. *Idili A., Amodio A., Vidonis M., Feinberg-Somerson J., Castronovo M., Ricci F.* (2014) Folding-upon-binding and signal-on electrochemical DNA sensor with high affinity and specificity. *Anal. Chem.*, **86**(18), 9013-9019. DOI: 10.1021/ac501418g
147. *Farzin L., Sadjadi S., Shamsipur M., Sheibani S.* (2020) Electrochemical genosensor based on carbon nanotube/amine-ionic liquid functionalized reduced graphene oxide nanoplatfor for detection of human papillomavirus (HPV16)-related head and neck cancer. *J. Pharm. Biomed. Anal.*, **179**, 112989. DOI: 10.1016/j.jpba.2019.112989
148. *Manzano M., Viezzi S., Mazerat S., Marks R.S., Vidic J.* (2018) Rapid and label-free electrochemical DNA biosensor for detecting hepatitis A virus. *Biosens. Bioelectron.*, **100**, 89-95. DOI: 10.1016/j.bios.2017.08.043
149. *Carinelli S., Kühnemund M., Nilsson M., Pividori M.I.* (2017) Yoctomole electrochemical genosensing of Ebola virus cDNA by rolling circle and circle to circle amplification. *Biosens. Bioelectron.*, **93**, 65-71. DOI: 10.1016/j.bios.2016.09.099
150. *Ilkhani H., Farhad S.* (2018) A novel electrochemical DNA biosensor for Ebola virus detection. *Anal. Biochem.*, **557**, 151-155. DOI: 10.1016/j.ab.2018.06.010
151. *Ciftci S., Cánovas R., Neumann F., Paulraj T., Nilsson M., Crespo G.A., Madaboosi N.* (2020) The sweet detection of rolling circle amplification: Glucose-based electrochemical genosensor for the detection of viral nucleic acid. *Biosens. Bioelectron.*, **151**, 112002. DOI: 10.1016/j.bios.2019.112002
152. *Alzate D., Cajigas S., Robledo S., Muskus C., Orozco J.* (2020) Genosensors for differential detection of Zika virus. *Talanta*, **210**, 120648. DOI: 10.1016/j.talanta.2019.120648
153. *Bartosik M., Jirakova L., Anton M., Vojtesek B., Hrstka R.* (2018) Genomagnetic LAMP-based electrochemical test for determination of high-risk HPV16 and HPV18 in clinical samples. *Anal. Chim. Acta*, **1042**, 37-43. DOI: 10.1016/j.aca.2018.08.020
154. *Ahangar L.E., Mehrgardi M.A.* (2017) Amplified detection of hepatitis B virus using an electrochemical DNA biosensor on a nanoporous gold platform. *Bioelectrochemistry*, **117**, 83-88. DOI: 10.1016/j.bioelechem.2017.06.006
155. *Srisomwat C., Teengam P., Chuaypen N., Tangkijvanich P., Vilaivan T., Chailapakul O.* (2020) Pop-up paper electrochemical device for label-free hepatitis B virus DNA detection. *Sensors Actuators B Chem.*, **316**, 128077. DOI: 10.1016/j.snb.2020.128077
156. *Malhotra B.D., Ali M.A.* (2018) Nanomaterials in Biosensors: Fundamentals and Applications. In: *Nanomaterials for Biosensors*, William Andrew Publishing, pp. 1-74. DOI: 10.1016/B978-0-323-44923-6.00001-7
157. *Zhao F., Cao L., Liang Y., Wu Z., Chen Z., Zeng R.* (2017) Label-free amperometric immunosensor based on graphene oxide and ferrocene-chitosan nanocomposites for detection of hepatitis B virus antigen. *J. Biomed. Nanotechnol.*, **13**(10), 1300-1308. DOI: 10.1166/jbn.2017.2415
158. *Wei S., Xiao H., Cao L., Chen Z.* (2020) A label-free immunosensor based on graphene oxide/Fe<sub>3</sub>O<sub>4</sub>/Prussian blue nanocomposites for the electrochemical determination of HBsAg. *Biosensors*, **10**(3), 24. DOI: 10.3390/bios10030024
159. *Trindade E.K.G., Dutra R.F.* (2018) A label-free and reagentless immunoelectrode for antibodies against hepatitis B core antigen (anti-HBc) detection. *Colloids Surfaces B Biointerfaces*, **172**, 272-279. DOI: 10.1016/j.colsurfb.2018.08.050
160. *Gao Z., Li Y., Zhang X., Feng J., Kong L., Wang P., Chen Z., Dong Y., Wei Q.* (2018) Ultrasensitive electrochemical immunosensor for quantitative detection of HBeAg using Au@Pd/MoS<sub>2</sub>@MWCNTs nanocomposite as enzyme-mimetic labels. *Biosens. Bioelectron.*, **102**, 189-195. DOI: 10.1016/j.bios.2017.11.032
161. *Alizadeh N., Hallaj R., Salimi A.* (2018) Dual amplified electrochemical immunosensor for hepatitis B virus surface antigen detection using hemin/G-quadruplex immobilized onto Fe<sub>3</sub>O<sub>4</sub>-AuNPs or (hemin-amino-rGO-Au) nanohybrid. *Electroanalysis*, **30**(3), 402-414. DOI: 10.1002/elan.201700727
162. *Alizadeh N., Hallaj R., Salimi A.* (2017) A highly sensitive electrochemical immunosensor for hepatitis B virus surface antigen detection based on Hemin/G-quadruplex horseradish peroxidase-mimicking DNAzyme-signal amplification. *Biosens. Bioelectron.*, **94**, 184-192. DOI: 10.1016/j.bios.2017.02.039
163. *Li F., Li Y., Feng J., Gao Z., Lv H., Ren X., Wei Q.* (2018) Facile synthesis of MoS<sub>2</sub>@Cu<sub>2</sub>O-Pt nanohybrid as enzyme-mimetic label for the detection of the hepatitis B surface antigen. *Biosens. Bioelectron.*, **100**, 512-518. DOI: 10.1016/j.bios.2017.09.048
164. *Biasotto G., Costa J.P.C., Costa P.I., Zaghete M.A.* (2019) ZnO nanorods-gold nanoparticle-based biosensor for detecting hepatitis C. *Appl. Phys. A*, **125**(12), 821. DOI: 10.1007/s00339-019-3128-1
165. *Valipour A., Roushani M.* (2017) Using silver nanoparticle and thiol graphene quantum dots nanocomposite as a substratum to load antibody for detection of hepatitis C virus core antigen: Electrochemical oxidation of riboflavin was used as redox probe. *Biosens. Bioelectron.*, **89**, 946-951. DOI: 10.1016/j.bios.2016.09.086
166. *Valipour A., Roushani M.* (2017) A glassy carbon immunoelectrode modified with vanadium oxide nanobelts for ultrasensitive voltammetric determination of the core antigen of hepatitis C virus. *Microchim. Acta*, **184**(11), 4477-4483. DOI: 10.1007/s00604-017-2449-z
167. *Valipour A., Roushani M.* (2017) TiO<sub>2</sub> nanoparticles doped with Celestine Blue as a label in a sandwich immunoassay for the hepatitis C virus core antigen using a screen printed electrode. *Microchim. Acta*, **184**(7), 2015-2022. DOI: 10.1007/s00604-017-2190-7
168. *Singh R., Hong S., Jang J.* (2017) Label-free detection of influenza viruses using a reduced graphene oxide-based electrochemical immunosensor integrated with a microfluidic platform. *Sci. Rep.*, **7**(1), 42771. DOI: 10.1038/srep42771
169. *Huang J., Xie Z., Xie Z., Luo S., Xie L., Huang L., Fan Q., Zhang Y., Wang S., Zeng T.* (2016) Silver nanoparticles coated graphene electrochemical sensor for the ultrasensitive analysis of avian influenza virus H7. *Anal. Chim. Acta*, **913**, 121-127. DOI: 10.1016/j.aca.2016.01.050
170. *Wu Z., Guo W.-J., Bai Y.-Y., Zhang L., Hu J., Pang D.-W., Zhang Z.-L.* (2018) Digital single virus electrochemical enzyme-linked immunoassay for ultrasensitive H7N9 avian influenza virus counting. *Anal. Chem.*, **90**(3), 1683-1690. DOI: 10.1021/acs.analchem.7b03281
171. *Sayhi M., Ouerghi O., Belgacem K., Arbi M., Tepeli Y., Ghram A., Anik Ü., Österlund L., Laouini D., Diouani M.F.* (2018) Electrochemical detection of influenza virus H9N2 based on both immunomagnetic extraction and gold catalysis using an immobilization-free screen printed carbon microelectrode. *Biosens. Bioelectron.*, **107**, 170-177. DOI: 10.1016/j.bios.2018.02.018

172. Yang Z.-H., Zhuo Y., Yuan R., Chai Y.-Q. (2016) A nanohybrid of platinum nanoparticles-porous ZnO-hemin with electrocatalytic activity to construct an amplified immunosensor for detection of influenza. *Biosens. Bioelectron.*, **78**, 321-327. DOI: 10.1016/j.bios.2015.10.073
173. Darwish N.T., Alrawi A.H., Sekaran S.D., Alias Y., Khor S.M. (2016) Electrochemical immunosensor based on antibody-nanoparticle hybrid for specific detection of the Dengue virus NS1 biomarker. *J. Electrochem. Soc.*, **163**(3), B19-B25. DOI: 10.1149/2.0471603jes
174. Kim J.H., Cho C.H., Ryu M.Y., Kim J.-G., Lee S.-J., Park T.J., Park J.P. (2019) Development of peptide biosensor for the detection of dengue fever biomarker, nonstructural 1. *PLoS One*, **14**(9), e0222144. DOI: 10.1371/journal.pone.0222144
175. Kanagavalli P., Veerapandian M. (2020) Opto-electrochemical functionality of Ru(II)-reinforced graphene oxide nanosheets for immunosensing of dengue virus non-structural 1 protein. *Biosens. Bioelectron.*, **150**, 111878. DOI: 10.1016/j.bios.2019.111878
176. Faria A.M., Mazon T. (2019) Early diagnosis of Zika infection using a ZnO nanostructures-based rapid electrochemical biosensor. *Talanta*, **203**, 153-160. DOI: 10.1016/j.talanta.2019.04.080
177. Chin S.F., Lim L.S., Pang S.C., Sum M.S.H., Perera D. (2017) Carbon nanoparticle modified screen printed carbon electrode as a disposable electrochemical immunosensor strip for the detection of Japanese encephalitis virus. *Microchim. Acta*, **184**(2), 491-497. DOI: 10.1007/s00604-016-2029-7
178. Hien H.T., Giang H.T., Trung T., van Tuan C. (2017) Enhancement of biosensing performance using a polyaniline/multiwalled carbon nanotubes nanocomposite. *J. Mater. Sci.*, **52**(3), 1694-1703. DOI: 10.1007/s10853-016-0461-z
179. Svalova T.S., Malysheva N.N., Bubekova A.K., Saigushkina A.A., Medvedeva M.V., Kozitsina A.N. (2020) Effect of the method for immobilizing receptor layer on the analytical characteristics of a label-free electrochemical immunosensor for the determination of measles antibodies. *J. Anal. Chem.*, **75**(2), 254-261. DOI: 10.1134/S106193482002015X
180. Tran L.T., Tran T.Q., Ho H.P., Chu X.T., Mai T.A. (2019) Simple label-free electrochemical immunosensor in a microchamber for detecting Newcastle disease virus. *J. Nanomater.*, **2019**, 1-9. DOI: 10.1155/2019/3835609
181. Hou Y.-H., Wang J.-J., Jiang Y.-Z., Lv C., Xia L., Hong S.-L., Lin M., Lin Y., Zhang Z.-L., Pang D.-W. (2018) A colorimetric and electrochemical immunosensor for point-of-care detection of enterovirus 71. *Biosens. Bioelectron.*, **99**, 186-192. DOI: 10.1016/j.bios.2017.07.035
182. Walls A.C., Park Y.-J., Tortorici M.A., Wall A., McGuire A.T., Velesler D. (2020) Structure, function, and antigenicity of the SARS-CoV-2 spike glycoprotein. *Cell*, **181**(2), 281-292.e6. DOI: 10.1016/j.cell.2020.02.058
183. Seo G., Lee G., Kim M.J., Baek S.-H., Choi M., Ku K.B., Lee C.-S., Jun S., Park D., Kim H.G., Kim S.-J., Lee J.-O., Kim B.T., Park E.C., Kim S.I. (2020) Rapid detection of COVID-19 causative virus (SARS-CoV-2) in human nasopharyngeal swab specimens using field-effect transistor-based biosensor. *ACS Nano*, **14**(4), 5135-5142. DOI: 10.1021/acsnano.0c02823
184. Tamborelli A., Mujica M.L., Gallay P., Vaschetti V., Reartes D., Delpino R., Bravo L., Bollo S., Rodriguez M., Rubianes M.D., Dalmaso P., Rivas G. (2023) Biosensing strategies for the detection of SARS-CoV-2 nucleic acids. *J. Pharm. Biomed. Anal.*, **232**, 115370. DOI: 10.1016/j.jpba.2023.115370
185. Yakoh A., Pimpitak U., Rengpipat S., Hirankarn N., Chailapakul O., Chaiyo S. (2021) Paper-based electrochemical biosensor for diagnosing COVID-19: Detection of SARS-CoV-2 antibodies and antigen. *Biosens. Bioelectron.*, **176**, 112912. DOI: 10.1016/j.bios.2020.112912
186. Agafonova L., Zhdanov D., Gladilina Y., Kanashenko S., Shumyantseva V. (2022) A pilot study on an electrochemical approach for assessing transient DNA transfection in eukaryotic cells. *J. Electroanal. Chem.*, **920**, 116635. DOI: 10.1016/j.jelechem.2022.116635
187. Brabec V., Mornstein V. (1980) Electrochemical behaviour of proteins at graphite electrodes. I. Electrooxidation of proteins as a new probe of protein structure and reactions. *Biochim. Biophys. Acta Protein Struct.*, **625**(1), 43-50. DOI: 10.1016/0005-2795(80)90106-3
188. Brabec V., Mornstein V. (1980) Electrochemical behaviour of proteins at graphite electrodes. *Biophys. Chem.*, **12**(2), 159-165. DOI: 10.1016/0301-4622(80)80048-2
189. Shumyantseva V., Bulko T., Kuzikov A., Masamrekh R., Archakov A. (2018) Analysis of L-tyrosine based on electrocatalytic oxidative reactions via screen-printed electrodes modified with multi-walled carbon nanotubes and nanosized titanium oxide (TiO<sub>2</sub>). *Amino Acids*, **50**(7), 823-829. DOI: 10.1007/s00726-018-2557-z

Received: 02. 09. 2023.  
 Revised: 15. 10. 2023.  
 Accepted: 19. 10. 2023.

**ПЕРСПЕКТИВЫ СОЗДАНИЯ ВАКЦИННЫХ ПРЕПАРАТОВ НОВОГО ТИПА НА ОСНОВЕ ПСЕВДОВИРУСНЫХ ЧАСТИЦ (НА ПРИМЕРЕ ВАКЦИНЫ ПРОТИВ ПОЛИОМИЕЛИТА)**

*Д.Д. Жданов<sup>1\*</sup>, Ю.Ю. Ивин<sup>1,2</sup>, А.Н. Шишпарёнок<sup>1</sup>, С.В. Краевский<sup>1</sup>, С.Л. Канащенко<sup>1</sup>, Л.Е. Агафонова<sup>1</sup>, В.В. Шумянцева<sup>1,3</sup>, О.В. Гнеденко<sup>1</sup>, А.Н. Пиняева<sup>1,2</sup>, А.А. Ковпак<sup>1</sup>, А.А. Ишмухаметов<sup>2</sup>, А.И. Арчаков<sup>1,3</sup>*

<sup>1</sup>Научно-исследовательский институт биомедицинской химии им. В.Н. Ореховича, 119121, Москва, ул. Погодинская, 10; \*эл. почта: zhdanovdd@mail.ru

<sup>2</sup>Федеральный научный центр исследований и разработки иммунобиологических препаратов им. М.П. Чумакова РАН,

108819, Москва, поселение Московский, посёлок Института полиомиелита, домовладение 8, корп. 1

<sup>3</sup>Российский национальный исследовательский медицинский университет им. Н.И. Пирогова, 117997, Москва, ул. Островитянова, 1

Традиционные противовирусные вакцины создаются с использованием химической инактивации вируса, чаще всего под действием формальдегида и β-пропиолактона. Данные подходы не оптимальны, поскольку негативно влияют на сохранность антигенных детерминант инактивированных частиц и требуют дополнительных стадий очистки. Наиболее перспективными для создания вакцин считают платформы на основе псевдовирусных частиц, то есть инактивированных вирусов, которые полностью сохранили наружную оболочку, при этом потеряв способность к размножению из-за разрушения генома. Облучение вирусов ускоренными электронами является оптимальным путём создания псевдовирусных частиц. В данной обзорной работе на примере вируса полиомиелита представлены основные алгоритмы, применимые для функциональной и структурной характеристики псевдовирусных частиц в процессе создания вакцинного препарата, а именно анализа степени разрушения генома и иммуногенности. Рассмотрена структура вируса полиомиелита и методы его инактивации. Для функциональной характеристики псевдовирусов предложены алгоритмы оценки остаточной инфекционности и иммуногенности. Подходы по анализу целостности генома, атомно-силовая и электронная микроскопия, поверхностно-плазмонный резонанс и биоэлектрохимические методы являются ключевыми для структурной характеристики псевдовирусных частиц. Применение описанных в настоящей работе алгоритмов, разработанных для вируса полиомиелита, позволит создать перспективные вакцины нового типа на основе псевдовирусных частиц и оперативно отвечать на вызовы при появлении новых вирусных инфекций.

*Полный текст статьи на русском языке доступен на сайте журнала (<http://pbmc.ibmc.msk.ru>).*

**Ключевые слова:** псевдовироз; полиомиелит; вакцина; инактивация; функциональная характеристика; структурная характеристика

**Финансирование.** Исследование выполнено за счёт гранта Российского научного фонда № 23-15-00471.

Поступила в редакцию: 02.09.2023; после доработки: 15.10.2023; принята к печати: 19.10.2023.